

Stress Analysis of Composite Plate with a Crack Approaching Circular Hole

By

Khushbu C. Panchal

09MME011



DEPARTMENT OF MECHANICAL ENGINEERING

INSTITUTE OF TECHNOLOGY

NIRMA UNIVERSITY

AHMEDABAD-382481

May 2011

Stress Analysis of Composite Plate with a Crack Approaching Circular Hole

Major Project

Submitted in partial fulfillment of the requirements

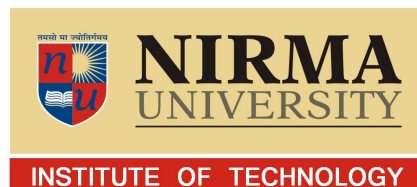
For the degree of

Master of Technology in Mechanical Engineering (CAD/CAM)

By

Khushbu C. Panchal

09MME011



DEPARTMENT OF MECHANICAL ENGINEERING

INSTITUTE OF TECHNOLOGY

NIRMA UNIVERSITY

AHMEDABAD-382481

May 2011

Declaration

This is to certify that

- i) The thesis comprises my original work towards the degree of Master of Technology in Mechanical Engineering (CAD/CAM) at Nirma University and has not been submitted elsewhere for a degree.
- ii) Due acknowledgement has been made in the text to all other material used.

Khushbu C. Panchal

Certificate

This is to certify that the Major Project entitled "Stress Analysis of Composite Plate with a Crack Approaching Circular Hole" submitted by Khushbu C. Panchal (09MME011), towards the partial fulfillment of the requirements for the degree of Master of Technology in Mechanical Engineering (CAD/CAM) of Nirma University of Science and Technology, Ahmedabad is the record of work carried out by her under my supervision and guidance. In my opinion, the submitted work has reached a level required for being accepted for examination. The results embodied in this major project, to the best of my knowledge, haven't been submitted to any other university or institution for award of any degree or diploma.

Dr. D.S. Sharma
Guide, Professor,
Department of Mechanical Engineering,
Institute of Technology,
Nirma University, Ahmedabad

Prof. V. R. Iyer
Professor and Head,
Department of Mechanical Engineering,
Institute of Technology,
Nirma University, Ahmedabad

Dr K Kotecha
Director,
Institute of Technology,
Nirma University, Ahmedabad

Acknowledgements

My deepest thanks to Prof. **Dr. D. S. Sharma** ,the guide of the project for guiding me with attention and care. I express my thanks to **Prof. V. R. Iyer**, the Head of the Department, Mechanical Engineering for extending his support.

I owe a great many thanks to a great many people those have helped and supported me directly or indirectly during my project work.

I would also thank my Institute and my faculty members without whom this project would have been a distant reality. I also thankful to seniors, colleagues for their support during critical analysis of the project. I also extend my heartfelt thanks to my family and well wishers.

- **Khushbu C. Panchal**

09MME011

Abstract

Composite laminated plates are being increasingly used in modern engineering applications, due to their high strength-to-weight and stiffness-to-weight ratios. Openings/cutouts are made into structures in order to satisfy some service requirements. These openings work as a stress raiser and may lead to the failure of the structure/machine component. When a structure is subjected to cyclic loads, cracks may initiate and grow in the vicinity of stress concentration. In order to ensure safety and reliability, it is necessary to predict the behavior of stress pattern around openings/cutouts under the application of various types of loading conditions.

In the present work, stress functions for a infinite composite laminated plate with crack approaching circular hole subjected to inplane loading have been obtained using Mushkelishvili's complex variable approach with the help of the conformal mapping and further the Schwarz's alternating method is used to solve the problem of the doubly connected region. Here an attempt is made to obtain the stress intensity factor at two crack tip for various crack length and interaction effect between crack and hole. The generalized stress function so obtained has been coded using MATLAB 7.6. Furthermore, the effect of various parameters such as loading conditions, fiber orientation angle, stacking sequence and material property on the stress functions have been studied. The different loading conditions considered here includes uniaxial, biaxial, or shear loading at infinity.

Keywords: *Composites, Complex variables, Conformal mapping, Stress function, Stress intensity factor.*

Contents

Declaration	iii
Certificate	iv
Acknowledgements	v
Abstract	vi
List of Tables	x
List of Figures	xi
Nomenclature	xiii
1 Introduction	1
1.1 Preliminary Remarks	1
1.2 Composite Materials	2
1.3 Mechanical Behavior of Composite Materials	3
1.4 Motivation	5
1.5 Aim and Scope of the Work	5
1.6 Methodology	5
1.7 Layout of the Report	6
2 Literature Review	8
2.1 Introduction	8
2.2 Single Hole Problem	8
2.3 Single Crack Problem	10
2.4 Interaction effect of two hole or hole and crack	10
2.5 Gaps Identified in the Literature	11
3 Complex Variable Formulation	12
3.1 Introduction	12
3.2 Analytical and Harmonic Functions	12
3.3 Conformal Mapping	13

3.4	Arbitrary Biaxial Loading Condition	14
3.5	General Solution for In-Plane Loading of laminates	16
3.6	Scheme of Solution for Single Hole	18
3.7	Interaction effect of Crack and Hole	20
4	Stress Analysis of Laminated Composite Plate	22
4.1	Preliminary Remarks	22
4.2	Stress Functions for Single Hole	22
4.2.1	First Stage	23
4.2.2	Second Stage	24
4.3	Stress Functions for Single Crack	26
4.3.1	First Stage	26
4.3.2	Second Stage	28
4.4	Stress Functions for Crack approaching Circular Hole Problem under Remote Loading	29
4.4.1	First Approximation	30
4.4.2	Second Approximation	30
4.4.3	Stress functions for hole	30
4.4.4	Stress functions for crack	34
4.4.5	Stress Intensity Factor	38
5	Results And Discussion	39
5.1	Preliminary Remarks	39
5.2	Methodology to Obtain Stress Field	39
5.3	Single Hole Problem	42
5.3.1	Stress Analysis of Isotropic Infinite Plate with Circular Hole	42
5.3.2	Stress Analysis of Anisotropic Infinite Plate with circular Hole	45
5.3.3	Stress Analysis of Isotropic plate with circular hole using ANSYS	48
5.3.4	Stress Analysis of Anisotropic plate with circular hole using ANSYS	49
5.3.5	Stress Analysis of Isotropic Infinite Plate with Elliptic Hole	51
5.3.6	Stress Analysis of Anisotropic Plate with Elliptic Hole	54
5.3.7	Stress Analysis of Isotropic plate with elliptical hole using ANSYS	57
5.3.8	Stress Analysis of Anisotropic plate with elliptical hole using ANSYS	58
5.4	Stress Analysis of Infinite Orthotropic plate with Crack	60
5.5	Crack Approaching Circular Hole Problem	62
5.5.1	Effect of Center Distance on Hole	62
5.5.2	Effect of Center Distance on Crack	67
5.6	Closing Remarks	72

<i>CONTENTS</i>	ix
6 Conclusion and Future Scope	73
6.1 Conclusion	73
6.2 Contributions of the Present Work	74
6.3 Limitations	74
6.4 Future Scope	74
A Compliance Coefficients	75
References	80

List of Tables

I	Material Properties for different materials use for numerical solution .	40
II	Complex parameter of anisotropy	41
III	Normalized Stress for different loading condition for isotropic Material plate with Circular Hole	43
IV	Normalized Stress for different loading condition for Anisotropic Material plate with Circular Hole	47
V	Comparison of results with results from ANSYS 11 for isotropic plate with circular hole	49
VI	Comparison of results with results from ANSYS 11 for anisotropic plate with circular hole	51
VII	Normalized Stress for different loading condition for Isotropic Material plate with Elliptical Hole	53
VIII	Normalized Stress for different loading condition for Anisotropic Material Plate with Elliptical Hole	55
IX	Comparison of results with results from ANSYS 11 for isotropic plate with elliptical hole	58
X	Comparison of results with results from ANSYS 11 for anisotropic plate with elliptical hole	60

List of Figures

3.1	Representation of Complex Variable	13
3.2	Conformal mapping	14
3.3	Arbitrary Biaxial Loading	15
3.4	The Curvilinear Co-ordinate System	18
3.5	The stages to solve problem of orthotropic plate with hole under remote loading	19
3.6	Orthotropic plate containing crack approaching hole subjected to remote loading	20
4.1	Orthotropic plate containing crack subjected to remote loading	26
5.1	Tangential Stress σ_θ/σ for isotropic material($\lambda=0$ for $\beta = 0$ and $\alpha = 0$)	43
5.2	Tangential Stress σ_θ/σ for isotropic material($\lambda=1$ for $\beta = 0$ and $\alpha = 0$)	44
5.3	Tangential Stress σ_θ/σ for isotropic material($\lambda = -1$ for $\beta = 45$ and $\alpha = 0$)	44
5.4	Tangential Stress σ_θ/σ for E-Glass/Epoxy($0/90$) _s ($\lambda=0, \beta = 0, \alpha = (0^\circ/90^\circ)_s$)	46
5.5	Tangential Stress σ_θ/σ for E-Glass/Epoxy($0/90$) _s ($\lambda=1, \beta = 0, \alpha = (0^\circ/90^\circ)_s$)	46
5.6	Tangential Stress σ_θ/σ for E-Glass/Epoxy($0/90$) _s ($\lambda = -1 \beta = 45 \alpha = (0^\circ/90^\circ)_s$)	47
5.7	Stress σ_y for isotropic material($\lambda=0$ for $\beta = 0$)	48
5.8	Stress σ_y for isotropic material($\lambda=1$)	49
5.9	Stress σ_y for E-Glass/Epoxy ($0/90$) _s ($\lambda=0$ for $\beta = 0$)	50
5.10	Stress σ_y for E-Glass/Epoxy ($0/90$) _s ($\lambda=1$)	50
5.11	Tangential Stress σ_θ/σ for isotropic material ($\lambda=0$ for $\beta = 0$ and $\alpha = 0$)	52
5.12	Tangential Stress σ_θ/σ for isotropic material($\lambda=1$ for $\beta = 0$ and $\alpha = 0$)	52
5.13	Tangential Stress σ_θ/σ for isotropic material($\lambda = -1$ for $\beta = 45$)	53
5.14	Tangential Stress σ_θ/σ for E-Glass/Epoxy ($0/90$) _s ($\lambda=0, \beta = 0, \alpha = (0^\circ/90^\circ)_s$)	55
5.15	Tangential Stress σ_θ/σ for E-Glass/Epoxy ($0/90$) _s ($\lambda=1, \alpha = (0^\circ/90^\circ)_s$)	56
5.16	Tangential Stress σ_θ for E-Glass/Epoxy ($0/90$) _s ($\lambda = -1 \beta = 45 \alpha = (0^\circ/90^\circ)_s$)	56

5.17	Stress σ_y for isotropic material ($\lambda=0$ for $\beta = 0$)	57
5.18	Stress σ_y for isotropic material($\lambda=1$)	58
5.19	Stress σ_y for E-Glass/Epoxy $(0/90)_s$ ($\lambda=0$ for $\beta = 0$)	59
5.20	Stress σ_y for E-Glass/Epoxy $(0/90)_s$ ($\lambda=1$)	59
5.21	Change in K_I/K_0 and K_{II}/K_0 with crack angle for Graphite/Epoxy (0/90)	61
5.22	Change in K_I/K_0 and K_{II}/K_0 with crack angle for Graphite/Epoxy (0/90) under shear load at infinity	61
5.23	Stress in Y-direction (σ_y) when plate is subjected to uniaxial loading ($\lambda = 0$) (E-Glass/Epoxy $[0/90]_s$)	63
5.24	Stress in Y-direction (σ_y) when plate is subjected to equi-biaxial loading($\lambda =$ 1) (E-Glass/Epoxy $[0/90]_s$)	63
5.25	Tangential Stress (σ_t) when plate is subjected to uniaxial loading($\lambda =$ 0) (E-Glass/Epoxy $[0/90]_s$)	64
5.26	Tangential Stress (σ_t) when plate is subjected to equi-biaxial loading($\lambda =$ 1) (E-Glass/Epoxy $[0/90]_s$)	64
5.27	Interaction effect between crack and hole ($C_0 = 5$) (E-Glass/Epoxy $[0/90]_s$)	65
5.28	Interaction effect between crack and hole ($C_0 = 3.5$) (E-Glass/Epoxy $[0/90]_s$)	65
5.29	Effect of center distance on normalized tangential stress on hole for crack length 4 (E-Glass/Epoxy $[0/90]_s$)	66
5.30	Effect of center distance on normalized tangential stress on hole for crack length 6 (E-Glass/Epoxy $[0/90]_s$)	66
5.31	normalized stress intensity factors for a crack approaching circular hole in cross ply laminate $[0_n/90_m]_s$ under uniform tensile stress ($d/R = 2$)	68
5.32	normalized stress intensity factors for a crack approaching circular hole in cross ply laminate $[0_n/90_m]_s$ under uniform tensile stress ($d/R = 3$)	68
5.33	normalized stress intensity factors for a crack approaching circular hole in cross ply laminate $[0_n/90_m]_s$ under uniform tensile stress ($d/R = 4$)	69
5.34	normalized stress intensity factors for a crack approaching circular hole in cross ply lamina $[0]$ under uniform tensile stress	69
5.35	normalized stress intensity factors for a crack approaching circular hole in cross ply laminate $[0_2/90]_s$ under uniform tensile stress	70
5.36	normalized stress intensity factors for a crack approaching circular hole in cross ply laminate $[0/90]_s$ under uniform tensile stress	70
5.37	Effect of center distance on stress intensity factor at crack tip B in cross ply laminate $[0/90]_s$ under uniform tensile stress	71
5.38	Effect of center distance on stress intensity factor at crack tip A in cross ply laminate $[0/90]_s$ under uniform tensile stress	71
A.1	Unidirectional Lamina	76
A.2	Geometry of multilayered laminate	76

Nomenclature

a_1, a_2, b_1, b_2	Constants related to anisotropy
a_3, a_4	Complex constants
a_{ij}	Elastic constant
f_1, f_2	First stage stress boundary conditions on the hole
f_1^0, f_2^0	Second stage stress boundary conditions on the hole
s_j	Complex parameter of anisotropic
z	Complex coordinate ($x + iy$)
z_j	Anisotropic complex coordinate
B, B', C'	Loading condition constants
C_0, C_1	Distance between two hole centers in mapped plane
$E_1, E_2, G_{12}, \nu_{12}$	Engineering constants of a lamina
Im	Imaginary part
K_I, K_{II}	Mode I and mode II stress intensity factor
L_1, L_2	Hole size constants
R_1, R_2	Hole radius in mm
Re	Real part
U	Air's stress function
Z_0	Centre distance between two holes in Z-plane
α	Fibre orientation angle
β_1, β_2	Orientation angle of loading
ν	Poisson's ratio
ϵ	Strain
ζ	Complex number in mapped plane
γ	Shear strain
τ	Shear stress, N/mm^2
σ	Stress, N/mm^2
$\sigma_{x'}^\infty, \sigma_{y'}^\infty, \tau_{xy'}^\infty$	Stresses at infinity
λ	Biaxial loading factor
λ_1, λ_2	Imaginary constants of Schwarz formula
$\omega(\zeta)$	Mapping function
$\phi(\zeta), \psi(\zeta)$	Complex potentials of the complex variables
$\phi'(\zeta), \psi'(\zeta)$	First derivative of complex function
$\phi''(\zeta), \psi''(\zeta)$	Second derivative of complex function

Chapter 1

Introduction

1.1 Preliminary Remarks

Composite materials, because of their high specific strength, stiffness and their flexible anisotropic property, have found a variety of applications in many engineering fields, such as in aerospace, automobiles and chemistry. As is known, holes and cutouts are inherent features and, in some cases, in the form of flaws in many engineering structures and these could cause serious problems of stress concentration due to the geometry discontinuity. Some composite materials are considered to be relatively brittle, therefore they are very sensitive to stress concentration and could fail easily when the applied load reaches the proportional limit.

Openings/cutouts are made into structures in order to satisfy some service requirements, results in strength degradation. In order to ensure safety and reliability, it is necessary to predict the behavior of openings/cutouts under the application of various types of loading conditions. In practice different shape of holes are used for different applications. For example manhole of any pressure vessel is either circular or elliptical while the window or door of an airplane is rectangular hole having chamfer of some radius at corners. The stress analysis of infinite plate with openings is interesting field of investigation.

The mechanism of fracture of a material in the microscale is closely associated with the interaction, coalescence, growth and propagation of minute defects such as cracks, voids and inclusions. The presence of a crack in the vicinity of a hole induces an interaction effect and hence the single crack solution becomes invalid. Various studies have been conducted to examine the stress concentrations around cutouts in infinite and finite dimensional anisotropic materials, and the failure strength. However relatively few studies of the problem of crack extension from areas of stress concentrations in anisotropic materials have been reported. Here an attempt is made to solve elastostatic problem of crack approaching circular hole in composite laminate using Muskhelishvili's complex variable approach.

In order to predict the behavior of the composite structure, it is essential to study the effect of anisotropy and type of loading on stress distribution around the openings and also the influence of two openings on each other. Analytical solutions give benchmarking results and such solutions for stress concentration problems are available in the literature for individual shape of holes in plates under specific case of loading. The present work is to derive the solutions for determining the stress intensity factor at crack tip and stress around hole in symmetric laminates under remotely applied inplane loads and also interaction effect between crack and hole on each other.

1.2 Composite Materials

A structural *composite*[1][2] is a material system consisting of two or more phases on a macroscopic scale, whose mechanical performance and properties are designed to be superior to those of the constitute materials acting independently. One of the phases is usually discontinuous, stiffer and stronger and is called the reinforcement, where as the less stiff and weaker phase is continuous and is called matrix. The properties improved by forming composite include stiffness, strength, weight reduction, corrosion resistance, fatigue life and wear resistance.

A *lamina* is a fundamental building block. A fiber-reinforced lamina consists of many

fibers embedded in matrix material, which can be metal, non-metal or thermo plastic polymer. Fibers can be unidirectional, bidirectional, discontinues or woven. The unidirectional fiber reinforced lamina gives highest strength in the direction of fibers but they have very low strength in the direction transverse to that.

A *laminate* is a collection of laminae stacked, to achieve desired thickness and stiffness. Unidirectional laminates will be very strong in one direction, but will result in poor properties in the opposite direction. These types of laminates are poor in shear also. A laminate is called *symmetric* when for each layer on one side of mid plane there is a corresponding layer at an equal distance from the mid plane. On the other side, it is with identical thickness, orientation, and properties. The laminate is symmetric in both geometry and material properties. Laminates that do not possess this property are known as *un-symmetric* laminates.

Because of the mismatch of the material properties between layers, and the shear stresses produced between layers may cause delamination. Also during manufacturing of the laminates, material defects such as inter laminar voids, incorrect orientation, damaged fibers, and variation in thickness may be introduced. It is impossible to remove such defects altogether. Therefore, analysis and design procedure should account for defects.

1.3 Mechanical Behavior of Composite Materials

In contrast to the more conventional engineering materials, the composite material are often both heterogeneous and non-isotropic (orthotropic or more generally anisotropic).

An orthotropic body has material properties those are different in three mutually perpendicular directions at a point in the body and, further have three mutually perpendicular planes of material symmetry.

An anisotropic body has material properties those are different in all directions at a point in the body and no planes of material property symmetry exist. However in

both orthotropic and anisotropic cases, the properties are a function of orientation at a point in the body.

For orthotropic materials, like isotropic materials, application of normal stress along principal material direction results in extension in the direction of applied stress and contraction in the perpendicular direction to the applied stress. Shear stress causes shearing deformation. Unlike the isotropic materials, the shear modulus is independent of other material properties.

For anisotropic materials, the application of normal stress leads not only to extension in the direction of the stress and contraction perpendicular to it, but also to shearing deformation. Conversely, shearing stress causes extension and contraction in addition to the distortion of shearing deformation. This coupling between both loading modes and both deformation modes, i.e. shear-extension coupling is also a characteristic of orthotropic materials subjected to normal stress in a non-principal material direction. In the formulation of constitutive equations of lamina, the following assumptions are made:

1. A lamina is a continuum.
2. A lamina behaves like a linear elastic material.

The second assumption implies that the generalized Hooke's law is valid. Also both assumptions can be removed if we consider micro mechanical constitutive model. The composite materials are inherently heterogeneous from the microscopic point of view. The generalized Hooke's law for an anisotropic material under isothermal condition can be written as $\sigma_i = C_{ij}\varepsilon_j$, where

σ_i = Stress components,

C_{ij} = Material co-efficient,

ε_j = Strain components.

1.4 Motivation

The existence of cracks around areas of stress concentration is critical in engineering structures. Therefore, solutions to the problem of such cracks should be useful to designers and experimental investigators. The presence of a crack in the vicinity of the hole induces an interaction effect and hence the single crack solution becomes invalid. To assist the design engineer when making an estimate of this interaction effect between crack and hole, is the motivation behind the present study.

1.5 Aim and Scope of the Work

The aim of the present work is to obtain the general solution for determining the stress analysis of composite plate with crack approaching circular hole and also include the solution for studying the interaction effect between crack and hole.

It is expected that these general solution will be useful to study the effect of type of loading, fiber orientation, laminate geometry, stacking sequence and distance between crack and hole on stress intensity factor and stresses around hole in anisotropic plate.

1.6 Methodology

The formulations given by Lekhnitskii[3] and Savin[4] on the basis of Muskhelishvili's[5] complex variable approach are considered for the general solution of in-plane loading. The arbitrary biaxial condition given by Gao[6] is introduced to avoid superposition. The complex potential for plate with traction free hole, due to remotely applied loading are determined in two stages. In the first stage, the stress functions are obtained for the hole free plate due to remotely applied loading. The boundary condition on the fictitious hole are then determined from these stress function. In the second stage, the plate with hole is applied by a negative of the boundary conditions on its hole boundary in the absence of the remote loading and potentials are obtained using

Schwarz's integral. The final stress function are obtained by superimposing solution of stage one and stage two.

$$\phi(\zeta) = \phi_1(\zeta) + \phi_0(\zeta)$$

$$\psi(\zeta) = \psi_1(\zeta) + \psi_0(\zeta)$$

$\phi_1(\zeta)$, $\psi_1(\zeta)$ represents stress functions for hole free plate while $\phi_0(\zeta)$, $\psi_0(\zeta)$ represents stress functions for plate having fictitious hole.

The interaction effect between crack and hole for the infinite orthotropic plate, subjected to various type of loading is studied in the form of complex stress functions using Schwarz's alternating method. The Schwarz's alternating method is applied to the doubly connected region as follows. The stress functions for the crack are transformed to the center of the hole by rotation and translation. The boundary condition at the hole boundary is determined by using transformed stress functions. This stress function does not satisfy the required boundary condition at the hole. Hence a new problem of hole subjected to a combination of the negative of this boundary condition and required boundary condition on the hole boundary is solved, which gives the corrected stress functions gives the required stress functions. The superposition of the transformed and corrected stress functions as required.

1.7 Layout of the Report

The work done for fulfilling the stated objectives has been reported systematically in following chapters of this report.

The chapter 2 presents literature review of literature available in area of stress analysis of infinite plate having circular hole/crack, under different loading conditions for both isotropic and anisotropic materials. Also the literature related to multiple discontinuity is present in this chapter.

Chapter 3 gives the complex variable formulation. The conformal mapping, arbitrary loading condition and general solution for in-plane loading are explained in this chapter.

Chapter 4 highlights detailed equations for single hole to obtain the stress around holes under in-plane loading and equation for crack and hole to obtain the stress intensity factor at crack tip and stress around hole under in-plane loading .

Chapter 5 presents the interaction effects between crack and hole in infinite orthotropic plate subjected to arbitrary biaxial load at infinity.

The conclusion and future scope of study are included in chapter 6.

The appendices given at the end will make the report self-contented.

Chapter 2

Literature Review

2.1 Introduction

Stress concentration problem are studied from last 110 years, however there is a huge scope for further research. The Muskhelishvili's complex variable approach has enabled the solution of many boundary value problem in a simple manner. Lekhnitskii and Savin solved different problems of stress around isotropic and anisotropic plates using Muskhelishvili's complex variable approach.

In order to gain insight in to available literature and to identify the scope of future work, the literature on stresses around holes and stress intensity factor at crack tip in isotropic and anisotropic plates relating to in-plane loads is reviewed.

2.2 Single Hole Problem

Simha and Mohapatra[7] studied the perturbation of mean boundary stress and its root mean square value due to evolution of shape. Nine different shapes are considered and hydrostatic tension, uniaxial tension and shear loading are considered in their study. A linear elastic analysis in this paper may not support the physics of change in shapes, but extending the ideas to a linear visco-elastic material is possible. He has given the mapping function which will transform the nine irregular shapes to a unit

circle by using Conformal Mapping. From his approach the mapping function is

$$z = m(\zeta) = R(\zeta + \frac{m_1}{\zeta} + \dots + \frac{m_9}{\zeta^9})$$

He has taken for circular hole $m_k = 0, k = 1 \text{ to } 9$

for elliptical hole, $m_1 = 1, m_k = 0, k = 2 \text{ to } 9$

for triangular hole, $m_3 = 1/3, m_k = 0, k = 2, k = 4 \text{ to } 9$

Gao[6] presented solution for infinite isotropic plate with elliptical hole. He introduced arbitrary biaxial loading condition to avoid superposition. By choosing appropriate biaxial loading factor λ , different type of loading condition at infinity can be applied. He has given the equation of stress

$$\sigma_x = \frac{P}{2}[(\lambda + 1) + (\lambda - 1) \cos 2\beta]$$

$$\sigma_y = \frac{P}{2}[(\lambda + 1) - (\lambda - 1) \cos 2\beta]$$

$$\tau_{xy} = \frac{P}{2}[(\lambda - 1) \sin 2\beta]$$

$\lambda = 0$ gives uniaxial loading and $\lambda = 1$ gives biaxial loading.

Ukadgaonker and Awasare[8][9] used the superposition principle, to obtain stress function for given plate by adding those of hole free plate under remote loading with a negative boundary condition on the fictitious hole together, ensuring the zero stress boundary condition on the hole. Uniaxial, biaxial and shear stresses are considered on isotropic plates containing circular, elliptical, triangular, and rectangular holes. Solution for biaxial and shear stresses are obtained by superposition of the solution of uniaxial loading.

Ukadgaonker and Rao[10] given generalized solution for irregular shaped hole in symmetric laminates under in plane loading using Savin's formulation for in plane (uniaxial loading, biaxial loading, shear at infinity, internal shear and internal pressure) loading problems. A general solution is developed by introducing a general form of mapping function and Gao's arbitrary biaxial loading conditions. Depending on the constants of the mapping function, biaxial loading factor, orientation angle and selection of appropriate values of the complex parameters of anisotropy, solution for the laminate, different laminate geometry is obtained.

Ukadgaonker and Kakhandki[11] found stress distribution around holes of differ-

ent shapes under different types of loading condition for symmetric infinite laminated composite plate using Kolosov-Muskhelishvili's complex variable approach. For load at infinity they adopted arbitrary biaxial loading factor describe by Gao[6].

D.S.Sharma[12] has given a solution for stress field around circular hole in infinite plate subjected to biaxial loading using complex variable approach. The stress functions are obtained by evaluating cauchy's integral formula for given boundary condition.

2.3 Single Crack Problem

D.S.Sharma [13] presented a solution for Stress analysis of infinite orthotropic plate with an arbitrarily oriented crack subjected to inplane loading at infinity. The effect of crack length, crack orientation and anisotropy on stress intensity factors is studied.

D.S.Sharma and Ukadgaonker[14] have given the general solution for determining the stress intensity factors, for cracks emanating from circular hole in laminated composite infinite plate subjected to arbitrary loading, with layers of arbitrary fiber orientations and stacking sequence, are obtained using Muskhelishvili's complex variable method.

2.4 Interaction effect of two hole or hole and crack

Ukadgaonker[15] has given the solution for the stress field produced in an isotropic homogeneous infinite plate with two unequal elliptical holes whose major axes coincide with the x-axis using Muskhelishvili's complex variable approach.

Ukadgaonker and Naik[16][17] have given the solution for an isotropic homogeneous infinite plate, with two arbitrarily oriented cracks of different lengths, subjected to uniform uniaxial tension at infinity. The problem is formulated in the complex

plane using the Muskhelishvili stress functions and further the Schwarz's alternating method is used to solve the problem of the doubly connected region.

Cheong and Kwon[18] obtained the stress intensity factor by using modified mapping collocation method which is based on analytic function theory of complex variables for problem of crack approaching two circular holes in $[0_n/90_m]_s$ laminates. They presented result for a crack approaching two circular holes in anisotropic infinite plate.

Lin and Ueng[19] have obtained the stresses in a laminated composite containing two identical elliptical holes is solved by the method of stress functions in terms of complex variables. They also studied the stress variation due to a change of the distance between the two holes, the size of the hole, as well as the laminate characteristic.

2.5 Gaps Identified in the Literature

- Most of the solutions available have considered uniaxial loading. Other cases of loading are obtained by superposition of the solutions of uniaxial loading.
- Solutions for the problem of anisotropic media subjected to doubly connected region has not been sufficiently addressed.
- Very few analytical solutions are available considering transverse shear deformation for plates containing holes in anisotropic plates.
- Crack approaching circular hole in anisotropic media is not addressed so far.

Chapter 3

Complex Variable Formulation

3.1 Introduction

Complex variable approach is a tool to handle the two dimensional problems. It can handle stress concentration, contact stress problem, fracture mechanics and fluid flow problems too. This formulation is based on two dimensional theory of elasticity using complex variable method dependent on Kolosov-Muskhelishvili's complex variable approach.

The motive of the formulation is to achieve the general solutions for thin laminates with single hole and two holes under in-plane loading. The problem of multiply connected region is solved by reducing it in to number of problems of simply connected regions, using Schwarz's alternating method. In-plane loading includes arbitrary bi-axial loading on hole boundary.

3.2 Analytical and Harmonic Functions

A complex number is represented as $z = x + iy$ and its conjugate is represented as $\bar{z} = x - iy$. Below Figure 3.1 shows representation in rectangular coordinate system. If $f(z) = u_1 + iv_1$ Where $u_1 = u_1(x, y)$ and $v_1 = v_1(x, y)$. and $f(z)$ is differentiable in any region S then it is called analytical function in the region S. If there is branch

or loop in the region then the function will fail to become analytical, those points where function is not analytical are called singular points. For a function of real variables x and y first and second order partial derivation are continuous and satisfy the partial differential equation then it is called harmonic function and in physics. it is considered as potential function.

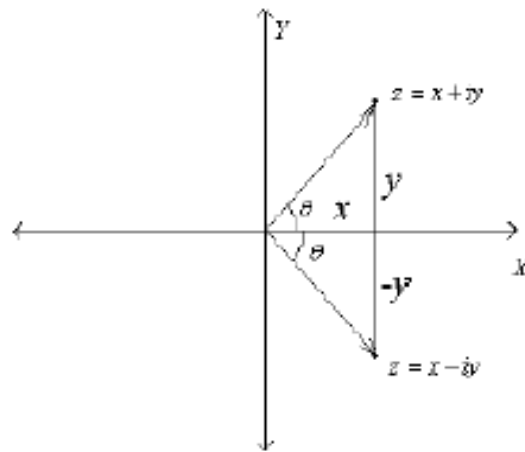


Figure 3.1: Representation of Complex Variable

3.3 Conformal Mapping

Conformal mappings are widely used in plane linear elasticity problems as they help in transforming very complicated shapes into simpler ones. While solving boundary value problems, though conformal mappings give more complex boundary conditions, it is preferred because of the simpler shapes it gives.

It facilitates representing the area external to a given hole in z -plane by the area outside the unit circle in ζ plane using a generalized transformation function given below.

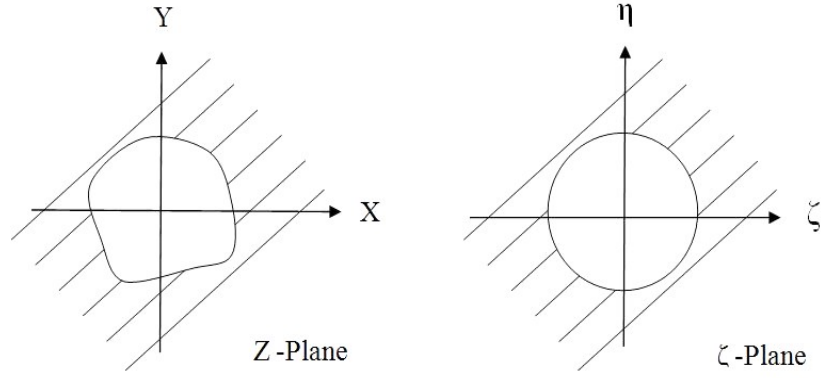


Figure 3.2: Conformal mapping

$$z = w(\zeta) = R(\zeta + \sum_{k=1}^N \frac{m_k}{\zeta^k})$$

where m_k are the constants of mapping function. N is the maximum number of terms.

Taking $\zeta = \rho e^{i\theta}$ where ρ, θ are the coordinates in ζ -plane and by taking $\rho = 1$ for the unit circle, and by introducing the complex parameter of anisotropy s_j in the previous equation, by affine transformation, z becomes,

$$z_j = w_j(\zeta) = R[(\cos \theta + \sum_{k=1}^N m_k \cos k\theta) + s_j[\sin \theta - \sum_{k=1}^N m_k \sin k\theta]]$$

The mapping function take the final form as:

$$z_j = w_j(\zeta) = \frac{R}{2}[a_j(\frac{1}{\zeta} + \sum_{k=1}^N m_k \zeta^k) + b_j(\zeta + \sum_{k=1}^N \frac{m_k}{\zeta^k})]$$

where, $a_j = (1 + is_j)$, $b_j = (1 - is_j)$, $(j = 1, \dots, 4)$

The complex parameters s_j depends upon material of laminate, type of loading and geometry. The complex parameter are obtained from characteristic equation of bi-harmonic equation for in-plane loading.

3.4 Arbitrary Biaxial Loading Condition

In order to consider several cases of in-plane loads the arbitrary loading conditions is introduced into the boundary conditions. This condition has been adapted from Gao's solution for elliptical hole in isotropic plate. By means of this conditions solution for biaxial loading can be obtained without the need of superposition of the solutions of

the Uniaxial loading. This can be achieved by introducing biaxial loading factor λ and the orientation angle β into the boundary conditions at infinity. An infinite plate with a hole and subjected to in-plane loading is shown in figure 3.3. The boundary conditions for different in-plane loading conditions are as follows:

$$\sigma_{x'}^{\infty} = \lambda\sigma ; \sigma_{y'}^{\infty} = \sigma ; \tau_{xy'}^{\infty} = 0 \text{ At } z \longrightarrow \infty \quad (3.1)$$

Where, $\sigma_{x'}^{\infty}$, $\sigma_{y'}^{\infty}$, stresses applied about x' , y' axes at infinity.

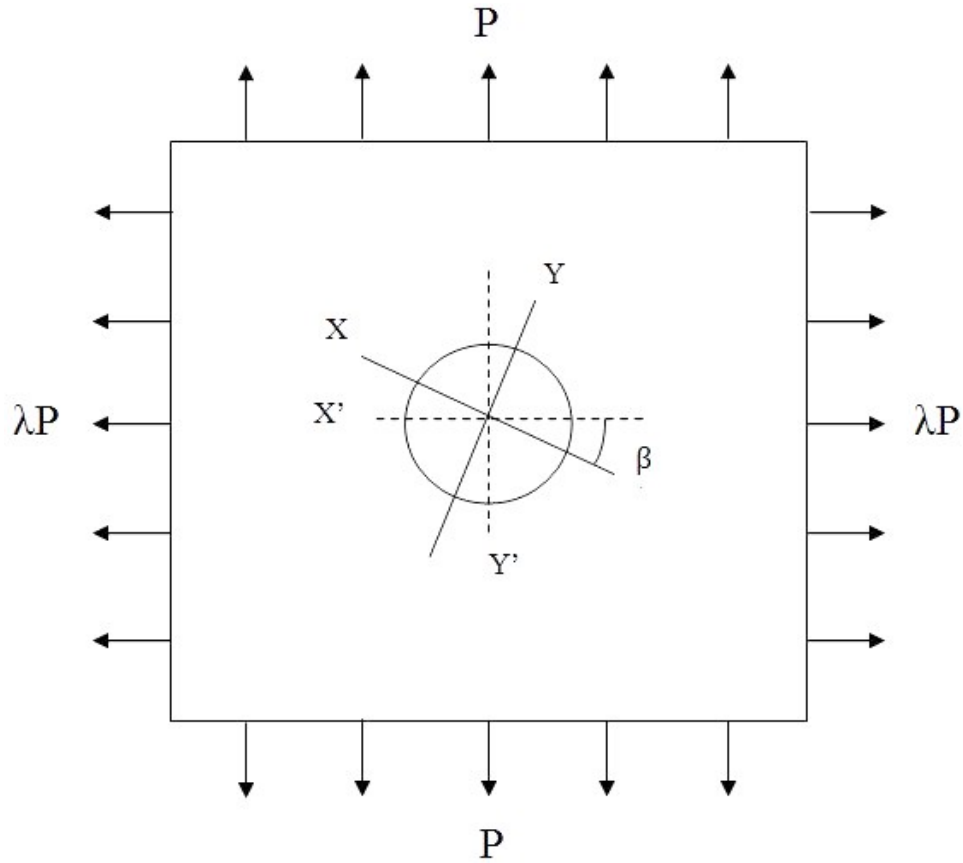


Figure 3.3: Arbitrary Biaxial Loading

By applying stress invariance into above boundary conditions, boundary conditions about XOY can be written explicitly as:

$$\begin{aligned}\sigma_x &= \frac{P}{2}[(\lambda + 1) + (\lambda - 1) \cos 2\beta] \\ \sigma_y &= \frac{P}{2}[(\lambda + 1) - (\lambda - 1) \cos 2\beta] \\ \tau_{xy} &= \frac{P}{2}[(\lambda - 1) \sin 2\beta]\end{aligned}\tag{3.2}$$

$\lambda=0$ and $\lambda=1$ explains uniaxial and biaxial loading conditions, respectively.

3.5 General Solution for In-Plane Loading of laminates

A thin anisotropic plate is considered under generalized plane stress condition. The plate is assumed to be loaded in such a way that resultant lies in XOY plane. The stresses on top and bottom surface of plate as well as σ_z , τ_{xz} , and τ_{yz} are zero everywhere within the plate. The mean values of strains along thickness of plate can be represented by generalized Hooke's law.

$$\begin{Bmatrix} \varepsilon_x \\ \varepsilon_y \\ \gamma_{xy} \end{Bmatrix} = \begin{bmatrix} a_{11} & a_{12} & a_{16} \\ a_{21} & a_{22} & a_{26} \\ a_{16} & a_{26} & a_{66} \end{bmatrix} \begin{Bmatrix} \sigma_x \\ \sigma_y \\ \tau_{xy} \end{Bmatrix}\tag{3.3}$$

Introducing Airy's stress function the stresses can be written as

$$\sigma_x = \frac{\partial^2 U}{\partial y^2}; \sigma_y = \frac{\partial^2 U}{\partial x^2}; \tau_{xy} = -\frac{\partial^2 U}{\partial x \partial y}\tag{3.4}$$

Substituting them in compatibility condition

$$\frac{\partial^2 \varepsilon_x}{\partial y^2} + \frac{\partial^2 \varepsilon_y}{\partial x^2} = \frac{\partial^2 \gamma_{xy}}{\partial x \partial y}\tag{3.5}$$

we get

$$a_{22} \frac{\partial^4 U}{\partial x^4} - 2a_{26} \frac{\partial^4 U}{\partial x^3 \partial y} + (2a_{12} + a_{66}) \frac{\partial^4 U}{\partial x^2 \partial y^2} - 2a_{16} \frac{\partial^4 U}{\partial x \partial y^3} + a_{11} \frac{\partial^4 U}{\partial y^4} = 0 \quad (3.6)$$

The general solution of above equation depends upon the roots of characteristic equation

$$a_{11}s^4 - 2a_{16}s^3 + (2a_{12} + a_{66})s^2 - 2a_{26}s + a_{22} = 0 \quad (3.7)$$

The roots of this equation are

$$\begin{aligned} s_1 &= \alpha_1 + i\beta_1, s_2 = \alpha_2 + i\beta_2 \\ s_3 &= \alpha_1 - i\beta_1, s_4 = \alpha_2 - i\beta_2 \end{aligned} \quad (3.8)$$

The Airy's stress function $U(x,y)$ can be represented as

$$\begin{aligned} U(x,y) &= F_1(x + D_1y) + F_2(x + D_2y) + F_3(x + D_3y) + F_4(x + D_4y) \\ U(x,y) &= F_1(z_1) + F_2(z_2) + \overline{F_1(z_1)} + \overline{F_2(z_2)} \end{aligned}$$

The analytic functions $\phi(z_1)$, $\psi(z_2)$ and their conjugates are given by

$$\frac{dF_1}{dz_1} = \phi(z_1); \quad \frac{dF_2}{dz_2} = \psi(z_2); \quad \frac{d\overline{F_1}}{d\overline{z_1}} = \overline{\phi(z_1)}; \quad \frac{d\overline{F_2}}{d\overline{z_2}} = \overline{\psi(z_2)}$$

By substituting analytic function into equation of Airy's stress function, and finally analytic function into equation(3.4), the stress components in terms of $\phi(z_1)$ and $\psi(z_2)$ can be represented as

$$\begin{aligned} \sigma_x &= 2Re[s_1^2 \phi'(z_1) + s_2^2 \psi'(z_2)] \\ \sigma_y &= 2Re[\phi'(z_1) + \psi'(z_2)] \\ \tau_{xy} &= -2Re[s_1 \phi'(z_1) + s_2 \psi'(z_2)] \end{aligned} \quad (3.9)$$

The stresses in Cartesian co-ordinates given in equation (3.9) can be represented in orthogonal curvilinear co-ordinates system by means of the following relations (Refer Figure [3.4])

$$\sigma_\theta + \sigma_\rho = \sigma_x + \sigma_y$$

$$\sigma_\theta - \sigma_\rho + 2i\tau_{\rho\theta} = (\sigma_y - \sigma_x + 2i\tau_{xy}) e^{2i\alpha}$$

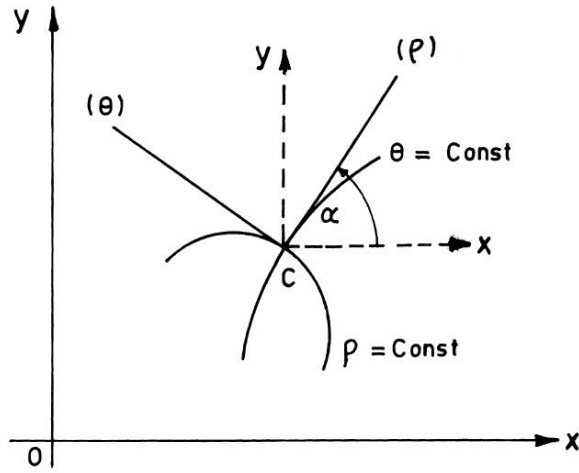


Figure 3.4: The Curvilinear Co-ordinate System

3.6 Scheme of Solution for Single Hole

The anisotropic plate containing a hole is subjected to remotely applied load is shown in figure 3.3. The edges of hole are free from loading. To obtain the solution, the problem is divided in two stages (Refer Figure [3.5])

First Stage: The stress functions $\phi_1(z_1)$, $\psi_1(z_2)$ are obtained for the hole free plate due to applied stresses σ_x^∞ , σ_y^∞ at infinity. The boundary condition f_1 and f_2 on the fictitious hole are then determined from these stress function.

Second Stage: For the second stage solution, the plate with hole is applied by a negative of the boundary condition ($f_1^0 = -f_1$ and $f_2^0 = -f_2$) on its hole boundary in the absence of remote loading. The stress functions of the second stage solution $\phi_0(z_1)$, $\psi_0(z_2)$ are obtained from these boundary conditions.

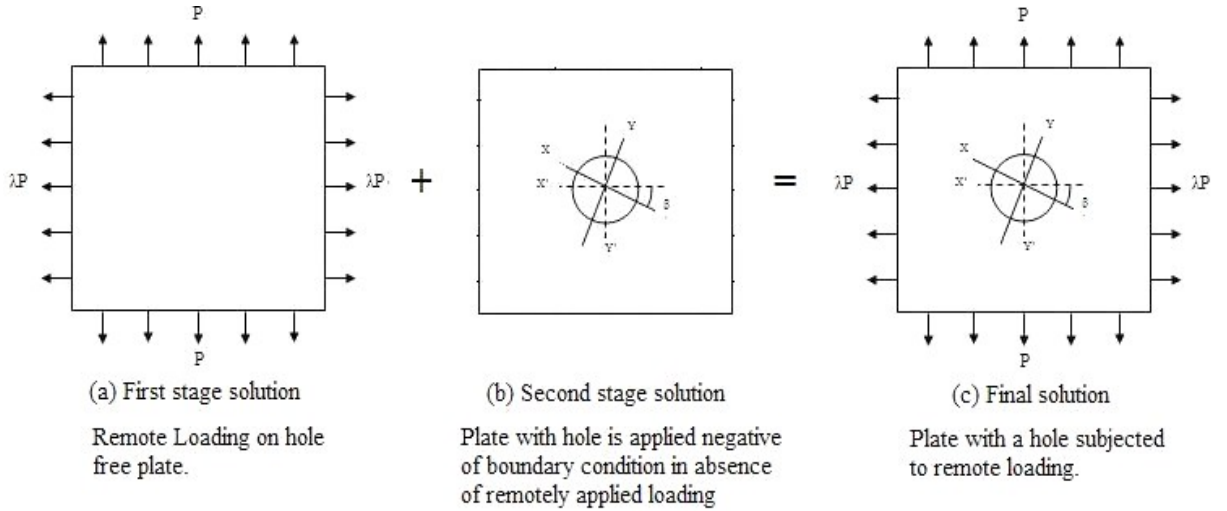


Figure 3.5: The stages to solve problem of orthotropic plate with hole under remote loading

Final Stage: The stress functions $\phi(z_1)$, $\psi(z_2)$ can be obtained by adding the stress functions of first and second stage.

$$\phi(z_1) = \phi_1(z_1) + \phi_0(z_1)$$

$$\psi(z_2) = \psi_1(z_2) + \psi_0(z_2)$$

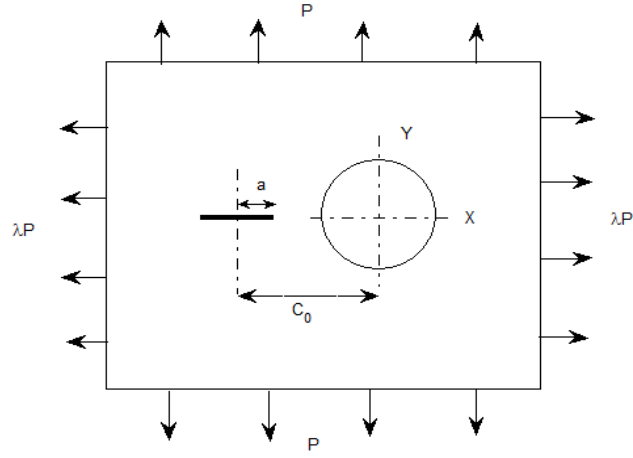


Figure 3.6: Orthotropic plate containing crack approaching hole subjected to remote loading

3.7 Interaction effect of Crack and Hole

The Figure [3.6] shows orthotropic laminated plate with crack approaching hole subjected to arbitrary biaxial load. a is half crack length, R_2 is hole radii, β_1 and β_2 are the angles with the direction of loads i.e. λP .

First Approximation The stress function for crack and hole are given by $\phi_1(\zeta_1)$; $\psi_1(\zeta_1)$ and $\phi_2(\zeta_2)$; $\psi_2(\zeta_2)$. This does not take any account of interaction effect of the other hole in the vicinity.

Second Approximation Starting from the crack to account interaction effect on hole the stress functions $\phi_1(\zeta_1)$; $\psi_1(\zeta_1)$ are transformed to the hole center O_2 by the rotation through angle $(\beta_1 + \beta_2)$ and translation through distance C_0 in mapped plane ζ - η .

The transformed stress functions are $\phi_{12}(\zeta_2)$ and $\psi_{12}(\zeta_2)$. This will be causing additional loading at the hole boundary. But the true loading condition at the hole is a stress free boundary condition. In order to achieve the stress free boundary condition at the hole, a new problem of an infinite plate with hole is solved with the negative boundary conditions. The corrected stress functions valid near the hole

$\phi_{22}(\zeta_2)$ and $\psi_{22}(\zeta_2)$ can be obtained.

The stress functions for the hole $\phi_2(\zeta_2)$ and $\psi_2(\zeta_2)$ can be obtained by superposition the corresponding transformed stress function $\phi_{12}(\zeta_2)$ and $\psi_{12}(\zeta_2)$.

$$\phi_2(\zeta_2) = \phi_{12}(\zeta_2) + \phi_{22}(\zeta_2)$$

$$\psi_2(\zeta_2) = \psi_{12}(\zeta_2) + \psi_{22}(\zeta_2)$$

Similarly, starting from the hole stress functions $\phi_2(\zeta_2)$ and $\psi_2(\zeta_2)$ the transformed and corrected stress functions are obtained as $\phi_{21}(\zeta_1)$; $\psi_{21}(\zeta_1)$, and $\phi_{11}(\zeta_1)$; $\psi_{11}(\zeta_1)$, respectively. The stress functions valid near the crack are

$$\phi_1(\zeta_1) = \phi_{21}(\zeta_1) + \phi_{11}(\zeta_1)$$

$$\psi_1(\zeta_1) = \psi_{21}(\zeta_1) + \psi_{11}(\zeta_1)$$

Chapter 4

Stress Analysis of Laminated Composite Plate

4.1 Preliminary Remarks

The infinite plate with crack approaching circular hole, subjected to biaxial loading is considered for interaction effect. The problem of doubly connected region is solved by reducing it to number of simply connected region.

In this chapter, stress function for single hole problem and crack approaching circular hole problem are obtained. This stress functions are used to calculate stress intensity factors and stress fields around hole.

4.2 Stress Functions for Single Hole

The anisotropic plate containing a hole is subjected to remotely applied load at outer edges as shown in Figure [3.3]. The edges of hole are free from loading. To determine the stress function; the solution is divided in to two stages:

4.2.1 First Stage

The stress functions $\phi_1(z_1)$ and $\psi_1(z_2)$ are obtained for hole free plate due to remotely applied load $\sigma_x^\infty, \sigma_y^\infty$.

$$\begin{aligned}\phi_1(z_1) &= Bz_1 \\ \psi_1(z_2) &= (B' + iC')z_2\end{aligned}\tag{4.1}$$

Where

$$\begin{aligned}B &= \frac{\sigma_x + (\alpha_2^2 + \Omega_2^2)\sigma_y + 2\alpha_2\tau_{xy}}{2[(\alpha_2 - \alpha_1)^2 + (\Omega_2^2 - \Omega_1^2)]}; \\ C &= 0; \\ B' &= \frac{-\sigma_x + (\alpha_1^2 - \Omega_1^2 - 2\alpha_1\alpha_2)\sigma_y - 2\alpha_2\tau_{xy}}{2[(\alpha_2 - \alpha_1)^2 + (\Omega_2^2 - \Omega_1^2)]}; \\ C' &= \frac{\sigma_x(\alpha_1 - \alpha_2) + (\alpha_2(\alpha_1^2 - \Omega_1^2) - \alpha_1(\alpha_2^2 - \Omega_2^2))\sigma_y + ((\alpha_1^2 - \Omega_1^2) - (\alpha_2^2 - \Omega_2^2))\tau_{xy}}{2\Omega_2[(\alpha_2 - \alpha_1)^2 + (\Omega_2^2 - \Omega_1^2)]}\end{aligned}\tag{4.2}$$

The boundary conditions f_1, f_2 on the fictitious hole are determined from these stress functions as follows

$$\begin{aligned}f_1 &= 2Re[\phi_1(z_1) + \psi_1(z_2)] \\ f_2 &= 2Re[s_1\phi_1(z_1) + s_2\psi_1(z_2)]\end{aligned}\tag{4.3}$$

Now consider the plate with hole and negative of the boundary conditions without external loading as shown in figure 3.4(b), the stress boundary condition on the hole are: $f_1^0 = -f_1$ $f_2^0 = -f_2$ and they are given by

$$\begin{aligned}f_1^0 &= -2Re[Bz_1 + (B' + iC')z_2] \\ f_2^0 &= -2Re[s_1Bz_1 + s_2(B' + iC')z_2]\end{aligned}\tag{4.4}$$

Upon introducing the mapping function in to boundary condition (4.4) we have

$$\begin{aligned} f_1^0 &= -[(K_1 + \overline{K_2}) \frac{1}{\zeta} + (K_2 + \overline{K_1})\zeta] \\ f_2^0 &= -[(K_3 + \overline{K_4}) \frac{1}{\zeta} + (K_4 + \overline{K_3})\zeta] \end{aligned} \quad (4.5)$$

Where

$$\begin{aligned} K_1 &= \frac{R}{2} [Ba_1 + (B' + iC') a_2], \\ K_2 &= \frac{R}{2} [Bb_1 + (B' + iC') b_2], \\ K_3 &= \frac{R}{2} [s_1 Ba_1 + s_2 (B' + iC') a_2], \\ K_4 &= \frac{R}{2} [s_1 Bb_1 + s_2 (B' + iC') b_2] . \end{aligned}$$

4.2.2 Second Stage

The plate with a hole is applied to negative of the boundary condition $f_1^0 = -f_1$ and $f_2^0 = -f_2$ in the absence of remote loading. The stress functions of second stage solution are obtained using these new boundary condition (f_1^0, f_2^0) into Schwarz formula:

$$\phi_0(\zeta) = \frac{i}{4\pi(s_1 - s_2)} \int_{\gamma} (s_2 f_1^0 - f_2^0) \frac{t + \zeta}{t - \zeta} \frac{dt}{t} + \lambda_1 \quad (4.6)$$

$$\psi_0(\zeta) = \frac{-i}{4\pi(s_1 - s_2)} \int_{\gamma} (s_1 f_1^0 - f_2^0) \frac{t + \zeta}{t - \zeta} \frac{dt}{t} + \lambda_2 \quad (4.7)$$

Where γ is a boundary of the unit circle in ζ -plane, t is the boundary value of ζ , λ_1 and λ_2 are imaginary constant which will have no contribution towards stress field and may be dropped here on.

By evaluating the integral the stress functions are obtained as

$$\begin{aligned}\phi_0 &= \left[\frac{a_3}{\zeta} \right] \\ \psi_0 &= - \left[\frac{a_4}{\zeta} \right]\end{aligned}\tag{4.8}$$

Where

$$\begin{aligned}a_3 &= \frac{1}{s_1 - s_2} \left[s_2 (K_1 + \overline{K_2}) - (K_3 + \overline{K_4}) \right] \\ a_4 &= \frac{1}{s_1 - s_2} \left[s_1 (K_1 + \overline{K_2}) - (K_3 + \overline{K_4}) \right]\end{aligned}$$

The stress functions $\phi(z_1)$, $\psi(z_2)$ for single hole problem, can be obtained by adding the stress functions of first and second stage.

$$\begin{aligned}\phi(z_1) &= \phi_1(z_1) + \phi_0(z_1) \\ \psi(z_2) &= \psi_1(z_2) + \psi_0(z_2)\end{aligned}\tag{4.9}$$

The stress around the hole in Cartesian co-ordinates can be written as follows:

$$\begin{aligned}\sigma_x &= \sigma_x^\infty + 2 \operatorname{Re} \left[s_1^2 \phi'_0(z_1) + s_2^2 \psi'_0(z_2) \right] \\ \sigma_y &= \sigma_x^\infty + 2 \operatorname{Re} \left[\phi'_0(z_1) + \psi'_0(z_2) \right] \\ \tau_{xy} &= \tau_{xy}^\infty - 2 \operatorname{Re} \left[s_1 \phi'_0(z_1) + s_2 \psi'_0(z_2) \right]\end{aligned}\tag{4.10}$$

Where,

$$\begin{aligned}\phi'_0(z_1) &= \frac{\phi'_0(\zeta)}{\omega'_1(\zeta)}; \psi'_0(z_2) = \frac{\psi'_0(\zeta)}{\omega'_2(\zeta)} \\ \omega'_1(\zeta) &= \frac{dz_1}{d\zeta}; \omega'_2(\zeta) = \frac{dz_2}{d\zeta}\end{aligned}\tag{4.11}$$

4.3 Stress Functions for Single Crack

The anisotropic plate containing a crack is subjected to remotely applied load at outer edges as shown in Figure [4.1]. The area external to a given crack, In Z-plane is mapped conformably to the area outside the unit circle in ζ plane using following mapping function.

$$z = w(\zeta) = R(\zeta + \frac{1}{\zeta})$$

Introducing the complex parameters s_j , and by affine transformation z becomes,

$$z = w(\zeta) = \frac{R}{2} (a_j + b_j) \left(\zeta + \frac{1}{\zeta} \right) \quad (4.12)$$

where R is a constant size of crack, $a_j = (1 + is_j)$, $b_j = (1 - is_j)$

To determine the stress function, the solution is divided into two stages:

4.3.1 First Stage

The stress functions $\phi_1(z_1)$ and $\psi_1(z_2)$ are obtained for hole free plate due to remotely applied load $\sigma_{x'}^\infty, \sigma_{y'}^\infty$.

$$\phi_1(z_1) = Bz_1$$

$$\psi_1(z_2) = (B' + iC')z_2 \quad (4.13)$$

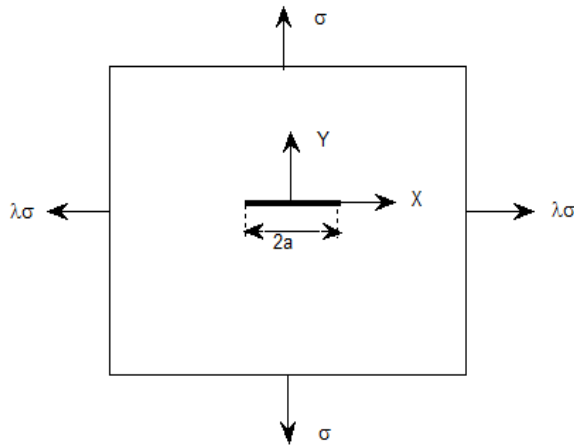


Figure 4.1: Orthotropic plate containing crack subjected to remote loading

Where

$$\begin{aligned}
 B &= \frac{\sigma_x + (\alpha_2^2 + \Omega_2^2) \sigma_y + 2\alpha_2 \tau_{xy}}{2 [(\alpha_2 - \alpha_1)^2 + (\Omega_2^2 - \Omega_1^2)]}, \\
 C &= 0; \\
 B' &= \frac{-\sigma_x + (\alpha_1^2 - \Omega_1^2 - 2\alpha_1 \alpha_2) \sigma_y - 2\alpha_2 \tau_{xy}}{2 [(\alpha_2 - \alpha_1)^2 + (\Omega_2^2 - \Omega_1^2)]}, \\
 C' &= \frac{\sigma_x (\alpha_1 - \alpha_2) + (\alpha_2 (\alpha_1^2 - \Omega_1^2) - \alpha_1 (\alpha_2^2 - \Omega_2^2)) \sigma_y + ((\alpha_1^2 - \Omega_1^2) - (\alpha_2^2 - \Omega_2^2)) \tau_{xy}}{2\Omega_2 [(\alpha_2 - \alpha_1)^2 + (\Omega_2^2 - \Omega_1^2)]} \quad (4.14)
 \end{aligned}$$

The boundary conditions f_1 , f_2 on the fictitious hole are determined from these stress functions as follows

$$\begin{aligned}
 f_1 &= 2Re[\phi_1(z_1) + \psi_1(z_2)] \\
 f_2 &= 2Re[s_1\phi_1(z_1) + s_2\psi_1(z_2)] \quad (4.15)
 \end{aligned}$$

By introducing the mapping function from equation (4.12)

$$\begin{aligned}
 f_1 &= 2Re[(K_1 + K_2) \left(\zeta + \frac{1}{\zeta} \right)] \\
 f_2 &= 2Re[(K_3 + K_4) \left(\zeta + \frac{1}{\zeta} \right)] \quad (4.16)
 \end{aligned}$$

where,

$$\begin{aligned}
 K_1 &= \frac{R}{2} [Ba_1 + (B' + iC') a_2], \\
 K_2 &= \frac{R}{2} [Bb_1 + (B' + iC') b_2], \\
 K_3 &= \frac{R}{2} [s_1Ba_1 + s_2(B' + iC') a_2], \\
 K_4 &= \frac{R}{2} [s_1Bb_1 + s_2(B' + iC') b_2] .
 \end{aligned}$$

4.3.2 Second Stage

The plate with a hole is applied to negative of the boundary condition $f_1^0 = -f_1$ and $f_2^0 = -f_2$ in the absence of remote loading. The stress functions of second stage solution are obtained using these new boundary condition (f_1^0, f_2^0) into Schwarz formula (Refer equation 4.6 and 4.7). By evaluating the integral the stress function are obtained as,

$$\begin{aligned}\phi_0 &= \left[\frac{a_3 + b_3}{\zeta} \right] \\ \psi_0 &= - \left[\frac{a_4 + b_4}{\zeta} \right]\end{aligned}\tag{4.17}$$

Where

$$\begin{aligned}a_3 &= \frac{1}{s_1 - s_2} \left[s_2 (K_1 + \overline{K_2}) - (K_3 + \overline{K_4}) \right] \\ a_4 &= \frac{1}{s_1 - s_2} \left[s_1 (K_1 + \overline{K_2}) - (K_3 + \overline{K_4}) \right] \\ b_3 &= \frac{1}{s_1 - s_2} \left[s_2 (K_2 + \overline{K_1}) - (K_4 + \overline{K_3}) \right] \\ b_4 &= \frac{1}{s_1 - s_2} \left[s_1 (K_2 + \overline{K_1}) - (K_4 + \overline{K_3}) \right]\end{aligned}$$

The stress functions $\phi(z_1), \psi(z_2)$ for single hole problem, can be obtained by adding the stress functions of first and second stage.

$$\begin{aligned}\phi(z_1) &= \phi_1(z_1) + \phi_0(z_1) \\ \psi(z_2) &= \psi_1(z_2) + \psi_0(z_2)\end{aligned}\tag{4.18}$$

The stress around the hole in Cartesian co-ordinates can be written as follows:

$$\begin{aligned}\sigma_x &= \sigma_x^\infty + 2 \operatorname{Re} \left[s_1^2 \phi_0'(z_1) + s_2^2 \psi_0'(z_2) \right] \\ \sigma_y &= \sigma_x^\infty + 2 \operatorname{Re} \left[\phi_0'(z_1) + \psi_0'(z_2) \right]\end{aligned}\tag{4.19}$$

$$\tau_{xy} = \tau_{xy}^{\infty} - 2 \operatorname{Re} [s_1 \phi'_0(z_1) + s_2 \psi'_0(z_2)]$$

Where,

$$\phi'_0(z_1) = \frac{\phi'_0(\zeta)}{\omega'_1(\zeta)}; \psi'_0(z_2) = \frac{\psi'_0(\zeta)}{\omega'_2(\zeta)}$$

$$\omega'_1(\zeta) = \frac{dz_1}{d\zeta}; \omega'_2(\zeta) = \frac{dz_2}{d\zeta}$$

The mode I and mode II stress intensity factors for the crack tips are obtained by using following formula given by Sih and Liebowitz[20],

$$K_I + \frac{K_{II}}{s_2} = 2\sqrt{\frac{\pi}{L}} \left(\frac{s_2 - s_1}{s_2} \right) \phi'(\zeta)$$

$$K_I + \frac{K_{II}}{s_1} = 2\sqrt{\frac{\pi}{L}} \left(\frac{s_1 - s_2}{s_1} \right) \psi'(\zeta)$$

4.4 Stress Functions for Crack approaching Circular Hole Problem under Remote Loading

In the Figure [3.6], a plate with crack approaching circular hole subjected to the arbitrary biaxial loading is shown. The size are constant for crack and hole are given by L_1 and L_2 respectively.

$$L_1 = \frac{R_1}{2}; L_2 = \frac{R_2}{2}$$

Where $R_1 = a/2$, where $2a$ is the crack length and R_2 is hole radii, β_1 and β_2 are the angles with the direction of loads i.e. λP .

Subscript '1' and '2' with symbol represents corresponding value of the parameter for crack and hole respectively.

4.4.1 First Approximation

The stress function for crack and hole are given by $\phi_1(\zeta_1)$; $\psi_1(\zeta_1)$ and $\phi_2(\zeta_2)$; $\psi_2(\zeta_2)$ respectively. This does not take any account of interaction effect of the other hole in the vicinity. Stress Function for crack

$$\begin{aligned}\phi_1(\zeta_1) &= \left[\frac{a_{31}}{\zeta_1} + \frac{b_{31}}{\zeta_1} \right] + B_1 \frac{L_1}{2} \left(\frac{a_1}{\zeta_1} + a_1\zeta_1 + b_1\zeta_1 + \frac{b_1}{\zeta_1} \right) \\ \psi_1(\zeta_1) &= - \left[\frac{a_{41}}{\zeta_1} + \frac{b_{41}}{\zeta_1} \right] + (B'_1 + iC'_1) \frac{L_1}{2} \left(\frac{a_2}{\zeta_1} + a_2\zeta_1 + b_2\zeta_1 + \frac{b_2}{\zeta_1} \right)\end{aligned}\quad (4.20)$$

Stress function for hole,

$$\begin{aligned}\phi_2(\zeta_2) &= \left[\frac{a_{32}}{\zeta_2} \right] + B_2 \frac{L_2}{2} \left(\frac{a_1}{\zeta_2} + b_1\zeta_2 \right) \\ \psi_2(\zeta_2) &= - \left[\frac{a_{41}}{\zeta_2} \right] + (B'_2 + iC'_2) \frac{L_2}{2} \left(\frac{a_2}{\zeta_2} + b_2\zeta_2 \right)\end{aligned}\quad (4.21)$$

4.4.2 Second Approximation

4.4.3 Stress functions for hole

The stress function $\phi_1(\zeta_1)$ and $\psi_1(\zeta_1)$ of the crack are transformed to the hole center O_2 by the rotation through angle $(\beta_1 + \beta_2)$ and translation through distance C_0 in the mapped plane, where C_0 is obtained from,

$$Z_0 = L_1 \left(C_0 + \frac{1}{C_0} \right) \quad (4.22)$$

Z_0 is the center distance between crack and hole in Z-plane,

Transferring the stress function to the center of hole

$$\phi_{12}(\zeta_2) = [\phi_1(\zeta_2 + C_0) e^{i(\beta_1 + \beta_2)}] e^{-i(\beta_1 + \beta_2)}$$

$$\psi_{12}(\zeta_2) = [\psi_1(\zeta_2 + C_0) e^{i(\beta_1 + \beta_2)}] e^{i(\beta_1 + \beta_2)} + \overline{C_0} \phi'_{12}(\zeta_2) \quad (4.23)$$

The transformed stress functions are

$$\begin{aligned} \phi_{12}(\zeta_1) &= \left[\frac{a_{31} + b_{31}}{(\zeta_2 + C_0) e^{2i(\beta_1 + \beta_2)}} \right] + B_1 \frac{L_1}{2} \left(\frac{(a_1 + b_1)}{(\zeta_2 + C_0) e^{2i(\beta_1 + \beta_2)}} \right) + (b_2 + a_2)(\zeta_2 + C_0) \\ \psi_{12}(\zeta_1) &= \left[- \left[\frac{(a_{41} + b_{41})}{(\zeta_2 + C_0)} \right] + (B'_1 + iC'_1) \frac{L_1}{2} \left(\frac{(a_2 + b_2)}{(\zeta_2 + C_0)} + (b_2 + a_2)(\zeta_2 + C_0) e^{2i(\beta_1 + \beta_2)} \right) \right] \\ &\quad + \left[\overline{C_0} \left[\frac{-(a_{31} + b_{31})}{(\zeta_2 + C_0)^2 e^{2i(\beta_1 + \beta_2)}} \right] \right] \\ &\quad + \overline{C_0} B_1 \frac{L_1}{2} \left(\frac{-(a_1 + b_1)}{(\zeta_2 + C_0)^2 e^{2i(\beta_1 + \beta_2)}} + (b_1 + a_1) \right) \end{aligned} \quad (4.24)$$

The transformed stress function gives a boundary condition f_1^{12} and f_2^{12} on the hole as

$$f_1^{12}(t_2) = [\phi_{12}(t_2) + \psi_{12}(t_2) + \overline{\phi_{12}(t_2)} + \overline{\psi_{12}(t_2)}] \quad (4.25)$$

$$f_2^{12}(t_2) = [s_1 \phi_{12}(t_2) + s_2 \psi_{12}(t_2) + \overline{s_1 \phi_{12}(t_2)} + \overline{s_2 \psi_{12}(t_2)}] \quad (4.26)$$

In order to achieve stress free boundary condition at the hole, a new problem of an infinite plate with hole is solved with boundary condition given by

$$f_1^{012} = -f_1^{12}(t_2); f_2^{012} = -f_2^{12}(t_2)$$

The corrected stress function near the hole are obtained using above boundary con-

ditions

$$\begin{aligned} \phi_{22}(\zeta_2) = & \frac{1}{s_2 - s_1} [N_{\phi 1} M_1 + N_{\phi 2} M_1 + N_{\phi 3} M_1 + N_{\phi 4} M_1 + N_{\phi 5} M_2 + N_{\phi 6} M_2] + \\ & \frac{1}{s_1 - s_2} [N_{\phi 7} + N_{\phi 8}] \end{aligned} \quad (4.27)$$

$$\begin{aligned} \psi_{22}(\zeta_2) = & \frac{1}{s_1 - s_2} [N_{\psi 1} M_1 + N_{\psi 2} M_1 + N_{\psi 3} M_1 + N_{\psi 4} M_1 + N_{\psi 5} M_2 + N_{\psi 6} M_2] + \\ & \frac{1}{s_1 - s_2} [N_{\psi 7} + N_{\psi 8}] \end{aligned} \quad (4.28)$$

Where,

$$\begin{aligned} N_{\phi 1} = & (\bar{s}_1 - s_2) (\bar{a}_{31} + \bar{b}_{31}) e^{2i(\beta_1 + \beta_2)} \\ N_{\phi 2} = & (\bar{s}_1 - s_2) B_1 \frac{L_1}{2} (\bar{a}_1 + \bar{b}_1) e^{2i(\beta_1 + \beta_2)} \\ N_{\phi 3} = & - (\bar{s}_2 - s_2) (\bar{a}_{41} + \bar{b}_{41}) \\ N_{\phi 4} = & (\bar{s}_2 - s_2) (B'_1 - iC'_1) \frac{L_1}{2} (\bar{a}_2 + \bar{b}_2) \\ N_{\phi 5} = & (\bar{s}_2 - s_2) (\bar{a}_{31} + \bar{b}_{31}) C_0 e^{2i(\beta_1 + \beta_2)} \\ N_{\phi 6} = & (\bar{s}_2 - s_2) B_1 \frac{L_1}{2} C_0 (\bar{a}_1 + \bar{b}_1) e^{-2i(\beta_1 + \beta_2)} \\ N_{\phi 7} = & - (\bar{s}_1 - s_2) B_1 \frac{L_1}{2} (\bar{b}_1 + \bar{a}_1) \frac{1}{\zeta_1} \\ N_{\phi 8} = & - (\bar{s}_2 - s_2) (B'_1 - iC'_1) \frac{L_1}{2} (\bar{b}_2 + \bar{a}_2) e^{-2i(\beta_1 + \beta_2)} \frac{1}{\zeta_1} \\ N_{\psi 1} = & (\bar{s}_1 - s_1) (\bar{a}_{31} + \bar{b}_{31}) e^{2i(\beta_1 + \beta_2)} \\ N_{\psi 2} = & (\bar{s}_1 - s_1) B_1 \frac{L_1}{2} (\bar{a}_1 + \bar{b}_1) e^{2i(\beta_1 + \beta_2)} \\ N_{\psi 3} = & - (\bar{s}_2 - s_1) (\bar{a}_{41} + \bar{b}_{41}) \\ N_{\psi 4} = & (\bar{s}_2 - s_1) (B'_1 - iC'_1) \frac{L_1}{2} (\bar{a}_2 + \bar{b}_2) \end{aligned}$$

$$N_{\psi 5} = (\overline{s_2} - s_1) (\overline{a_{31}} + \overline{b_{31}}) C_0 e^{2i(\beta_1 + \beta_2)}$$

$$N_{\psi 6} = (\overline{s_2} - s_1) B_1 \frac{L_1}{2} C_0 (\overline{a_1} + \overline{b_1}) e^{-2i(\beta_1 + \beta_2)}$$

$$N_{\psi 7}^* = (\overline{s_1} - s_1) B_2 \frac{L_2}{2} (\overline{b_1} + \overline{a_1}) \frac{1}{\zeta_1}$$

$$N_{\psi 8} = (\overline{s_2} - s_1) (B'_1 - iC'_1) \frac{L_1}{2} (\overline{b_2} + \overline{a_2}) e^{-2i(\beta_1 + \beta_2)} \frac{1}{\zeta_1}$$

$$M_1 = \left(\frac{1}{2\overline{C_0}} - \frac{1}{\overline{C_0}(1 + \zeta_2\overline{C_0})} \right)$$

$$M_2 = \left(\frac{1}{2\overline{C_0}^2} - \frac{1 + 2\zeta_2\overline{C_0}}{\overline{C_0}^2(1 + \zeta_2\overline{C_0})^2} \right)$$

The stress functions for the hole $\phi_2(\zeta_2)$ and $\psi_2(\zeta_2)$ are obtained by superposition of the corresponding transformed stress function onto corrected stress functions.

$$\phi_2(\zeta_2) = \phi_{12}(\zeta_2) + \phi_{22}(\zeta_2)$$

$$\psi_2(\zeta_2) = \psi_{12}(\zeta_2) + \psi_{22}(\zeta_2) \quad (4.29)$$

The derivatives of $\phi_2(\zeta_2)$ and $\psi_2(\zeta_2)$ are written as

$$\begin{aligned} \phi_2'(\zeta_2) = & \frac{1}{s_1 - s_2} [N_{\phi 1}M'_1 + N_{\phi 2}M'_1 + N_{\phi 3}M'_1 + N_{\phi 4}M'_1 + N_{\phi 5}M'_2 + N_{\phi 6}M'_2] + \\ & \frac{1}{s_1 - s_2} [N'_{\phi 7} + N'_{\phi 8}] + N'_{\phi 9} + N'_{\phi 10} \end{aligned} \quad (4.30)$$

$$\begin{aligned} \psi_2'(\zeta_2) = & \frac{1}{s_2 - s_1} [N_{\psi 1}M'_1 + N_{\psi 2}M'_1 + N_{\psi 3}M'_1 + N_{\psi 4}M'_1 + N_{\psi 5}M'_2 + N_{\psi 6}M'_2] + \\ & \frac{1}{s_1 - s_2} [N'_{\psi 7} + N'_{\psi 8}] + N'_{\psi 9} + N'_{\psi 10} \end{aligned} \quad (4.31)$$

$$\begin{aligned}
 N'_{\phi 7} &= (\bar{s}_1 - s_2) B_1 \frac{L_1}{2} \overline{(b_1 + a_1)} \frac{1}{\zeta_2^2} \\
 N'_{\phi 8} &= (\bar{s}_2 - s_2) (B'_1 - iC'_1) \frac{L_1}{2} \overline{(b_2 + a_2)} e^{-2i(\beta_1 + \beta_2)} \frac{1}{\zeta_2^2} \\
 N'_{\phi 9} &= - \left[\frac{(a_{31} + b_{31})}{(\zeta_2 + C_0)^2 e^{2i(\beta_1 + \beta_2)}} \right] \\
 N'_{\phi 10} &= B_1 \frac{L_1}{2} \left(\frac{-(a_1 + b_1)}{(\zeta_2 + C_0)^2 e^{2i(\beta_1 + \beta_2)}} + (b_1 + a_1) \right) \\
 N'_{\psi 7} &= - (\bar{s}_1 - s_1) B_1 \frac{L_1}{2} \overline{(b_1 + a_1)} \frac{1}{\zeta_2^2} \\
 N'_{\psi 8} &= - (\bar{s}_2 - s_1) (B'_1 - iC'_1) \frac{L_1}{2} \overline{(b_2 + a_2)} e^{-2i(\beta_1 + \beta_2)} \frac{1}{\zeta_2^2} \\
 N'_{\psi 9} &= \left[\left[\frac{(a_{41} + b_{41})}{(\zeta_2 + C_0)^2} \right] + (B'_1 + iC'_1) \frac{L_1}{2} \left(\frac{-(a_2 + b_2)}{(\zeta_2 + C_0)^2} + (b_2 + a_2) e^{2i(\beta_1 + \beta_2)} \right) \right] \\
 N'_{\psi 10} &= \left[2\bar{C}_0 \left[\frac{(a_{31} + b_{31})}{(\zeta_2 + C_0)^3 e^{2i(\beta_1 + \beta_2)}} \right] + 2\bar{C}_0 B_1 \frac{L_1}{2} \left(\frac{(a_1 + b_1)}{(\zeta_2 + C_0)^3 e^{2i(\beta_1 + \beta_2)}} \right) \right] \\
 M'_1 &= \left(\frac{1}{(1 + \zeta_2 \bar{C}_0)^2} \right) \\
 M'_2 &= \left(\frac{2\zeta_2}{(1 + \zeta_2 \bar{C}_0)^3} \right)
 \end{aligned}$$

4.4.4 Stress functions for crack

The stress function $\phi_2(\zeta_2)$ and $\psi_2(\zeta_2)$ of the hole are transformed to the crack center O_1 by the rotation through angle $-(\beta_1 + \beta_2)$ and translation through distance C_1 in the mapped plane, where C_1 is obtained from,

$$Z_0 = L_2(C_1) \quad (4.32)$$

Z_0 is the center distance between two holes in Z-plane,

Transferring the stress function to the center of the crack,

$$\begin{aligned}\phi_{21}(\zeta_1) &= [\phi_2(\zeta_1 - C_1) e^{-i(\beta_1 + \beta_2)}] e^{i(\beta_1 + \beta_2)} \\ \psi_{21}(\zeta_1) &= [\psi_2(\zeta_1 - C_1) e^{-i(\beta_1 + \beta_2)}] e^{-i(\beta_1 + \beta_2)} - \overline{C_1} \phi'_{21}(\zeta_1)\end{aligned}\quad (4.33)$$

The transformed stress functions are

$$\begin{aligned}\phi_{21}(\zeta_1) &= \left[\frac{a_{32}}{(\zeta_1 - C_1) e^{-2i(\beta_1 + \beta_2)}} \right] + B_2 \frac{L_2}{2} \left(\frac{a_1}{(\zeta_1 - C_1) e^{-2i(\beta_1 + \beta_2)}} + b_1(\zeta_1 - C_1) \right) \\ \psi_{21}(\zeta_1) &= \left[- \left[\frac{a_{42}}{(\zeta_1 - C_1)} \right] + (B'_2 + iC'_2) \frac{L_2}{2} \left(\frac{a_2}{(\zeta_1 - C_1)} + b_2(\zeta_1 - C_1) e^{-2i(\beta_1 + \beta_2)} \right) \right] \\ &\quad + \left[\overline{C_1} \left[\frac{a_{32}}{(\zeta_1 - C_1)^2 e^{-2i(\beta_1 + \beta_2)}} \right] + \overline{C_1} B_2 \frac{L_2}{2} \left(\frac{a_1}{(\zeta_1 - C_1)^2 e^{-2i(\beta_1 + \beta_2)}} + b_1 \right) \right]\end{aligned}\quad (4.34)$$

The transformed stress function gives a boundary condition $f_1^{21}(t_1)$ and $f_2^{21}(t_2)$ on the second hole as

$$f_1^{21}(t_1) = [\phi_{21}(t_1) + \psi_{21}(t_1) + \overline{\phi_{21}(t_1)} + \overline{\psi_{21}(t_1)}] \quad (4.35)$$

$$f_2^{21}(t_1) = [s_1 \phi_{21}(t_1) + s_2 \psi_{21}(t_1) + \overline{s_1} \overline{\phi_{21}(t_1)} + \overline{s_2} \overline{\psi_{21}(t_1)}] \quad (4.36)$$

In order to achieve stress free boundary condition at the crack, a new problem of an infinite plate with crack is solved with boundary condition given by

$$f_1^{0\ 21}(t_1) = -f_1^{21}(t_1); f_2^{0\ 21}(t_1) = -f_2^{21}(t_1)$$

The corrected stress function near the crack are obtained using above boundary con-

ditions

$$\begin{aligned} \phi_{11}(\zeta_1) = & \frac{1}{s_2 - s_1} [N_{\phi 1}^* M_{11}^* + N_{\phi 2}^* M_{12}^* + N_{\phi 3}^* M_{13}^* + N_{\phi 4}^* M_{14}^* + N_{\phi 5}^* M_{15}^* + \\ & \frac{1}{s_1 - s_2} [N_{\phi 6}^* M_{21}^* + N_{\phi 7}^* + N_{\phi 8}^*] \end{aligned} \quad (4.37)$$

$$\begin{aligned} \psi_{11}(\zeta_1) = & \frac{1}{s_1 - s_2} [N_{\psi 1}^* M_{11}^* + N_{\psi 2}^* M_{12}^* + N_{\psi 3}^* M_{13}^* + N_{\psi 4}^* M_{14}^* + N_{\psi 5}^* M_{15}^* + \\ & \frac{1}{s_1 - s_2} [N_{\psi 6}^* M_{21}^* + N_{\psi 7}^* + N_{\psi 8}^*] \end{aligned} \quad (4.38)$$

Where,

$$\begin{aligned} N_{\phi 1}^* &= (\bar{s}_1 - s_2) (\bar{a}_{32}) e^{-2i(\beta_1 + \beta_2)} \\ N_{\phi 2}^* &= (\bar{s}_1 - s_2) B_2 \frac{L_2}{2} (\bar{a}_1) e^{-2i(\beta_1 + \beta_2)} \\ N_{\phi 3}^* &= -(\bar{s}_2 - s_2) (\bar{a}_{42}) \\ N_{\phi 4}^* &= (\bar{s}_2 - s_2) (B'_2 - iC'_2) \frac{L_2}{2} (\bar{a}_2) \\ N_{\phi 5}^* &= (\bar{s}_2 - s_2) (\bar{a}_{32}) C_1 e^{-2i(\beta_1 + \beta_2)} \\ N_{\phi 6}^* &= (\bar{s}_2 - s_2) B_2 \frac{L_2}{2} C_1 (\bar{a}_1) e^{-2i(\beta_1 + \beta_2)} \\ N_{\phi 7}^* &= -(\bar{s}_1 - s_2) B_2 \frac{L_2}{2} (\bar{b}_1) \frac{1}{\zeta_1} \\ N_{\phi 8}^* &= -(\bar{s}_2 - s_2) (B'_2 - iC'_2) \frac{L_2}{2} (\bar{b}_2) e^{2i(\beta_1 + \beta_2)} \frac{1}{\zeta_1} \\ N_{\psi 1}^* &= (\bar{s}_1 - s_1) (\bar{a}_{32}) e^{-2i(\beta_1 + \beta_2)} \\ N_{\psi 2}^* &= (\bar{s}_1 - s_1) B_2 \frac{L_2}{2} (\bar{a}_1) e^{-2i(\beta_1 + \beta_2)} \\ N_{\psi 3}^* &= -(\bar{s}_2 - s_1) (\bar{a}_{42}) \\ N_{\psi 4}^* &= (\bar{s}_2 - s_1) (B'_2 - iC'_2) \frac{L_2}{2} (\bar{a}_2) \end{aligned}$$

$$\begin{aligned}
 N^*_{\psi 5} &= (\overline{s_2} - s_1) (\overline{a_{32}}) C_1 e^{-2i(\beta_1 + \beta_2)} \\
 N^*_{\psi 6} &= (\overline{s_2} - s_1) B_2 \frac{L_2}{2} C_1 (\overline{a_1}) e^{-2i(\beta_1 + \beta_2)} \\
 N^*_{\psi 7} &= (\overline{s_1} - s_1) B_2 \frac{L_2}{2} (\overline{b_1}) \frac{1}{\zeta_1} \\
 N^*_{\psi 8} &= (\overline{s_2} - s_1) (B'_2 - iC'_2) \frac{L_2}{2} (\overline{b_2}) e^{2i(\beta_1 + \beta_2)} \frac{1}{\zeta_1} \\
 M^*_1 &= \left(\frac{-1}{2\overline{C_1}} + \frac{1}{\overline{C_1}(1 - \zeta_1\overline{C_1})} \right); \\
 M^*_2 &= \left(\frac{1}{2\overline{C_1}^2} - \frac{1 - 2\zeta_1\overline{C_1}}{\overline{C_1}^2(1 - \zeta_1\overline{C_1})^2} \right)
 \end{aligned}$$

The stress functions for the crack $\phi_1(\zeta_1)$ and $\psi_1(\zeta_1)$ are obtained by superposition of the corresponding transformed stress function onto corrected stress functions.

$$\begin{aligned}
 \phi_1(\zeta_1) &= \phi_{21}(\zeta_1) + \phi_{11}(\zeta_1) \\
 \psi_1(\zeta_1) &= \psi_{21}(\zeta_1) + \psi_{11}(\zeta_1)
 \end{aligned} \tag{4.39}$$

The derivatives of $\phi_1(\zeta_1)$ and $\psi_1(\zeta_1)$ are written as

$$\begin{aligned}
 \phi_1'(\zeta_1) &= \frac{1}{s_2 - s_1} [N^*_{\phi 1} M'^*_{11} + N^*_{\phi 2} M'^*_{11} + N^*_{\phi 3} M'^*_{11} + N^*_{\phi 4} M'^*_{11} + N^*_{\phi 5} M'^*_{21}] + \\
 &\quad \frac{1}{s_1 - s_2} [N^*_{\phi 6} M'^*_{21} + N'^*_{\phi 7} + N'^*_{\phi 8}] + N'^*_{\phi 9} + N'^*_{\phi 10}
 \end{aligned} \tag{4.40}$$

$$\begin{aligned}
 \psi_1'(\zeta_1) &= \frac{1}{s_1 - s_2} [N^*_{\psi 1} M'^*_{11} + N^*_{\psi 2} M'^*_{11} + N^*_{\psi 3} M'^*_{11} + N^*_{\psi 4} M'^*_{11} + N^*_{\psi 5} M'^*_{21}] + \\
 &\quad \frac{1}{s_1 - s_2} [N^*_{\psi 6} M'^*_{21} + N'^*_{\psi 7} + N'^*_{\psi 8}] + N'^*_{\psi 9} + N'^*_{\psi 10}
 \end{aligned} \tag{4.41}$$

$$N'^*_{\phi 7} = (\overline{s_1} - s_2) B_2 \frac{L_2}{2} (\overline{b_1}) \frac{1}{\zeta_1^2}$$

$$N'^*_{\phi 8} = (\bar{s}_2 - s_2) (B'_2 - iC'_2) \frac{L_2}{2} (\bar{b}_2) e^{2i(\beta_1 + \beta_2)} \frac{1}{\zeta_1^2}$$

$$N'^*_{\phi 9} = - \left[\frac{(a_{32})}{(\zeta_1 - C_1)^2 e^{-2i(\beta_1 + \beta_2)}} \right]$$

$$N'^*_{\phi 10} = B_2 \frac{L_2}{2} \left(\frac{(-a_1)}{(\zeta_2 + C_0)^2 e^{-2i(\beta_1 + \beta_2)}} + (b_1) \right)$$

$$N'^*_{\psi 7} = - (\bar{s}_1 - s_1) B_2 \frac{L_2}{2} (\bar{b}_1) \frac{1}{\zeta_1^2}$$

$$N'^*_{\psi 8} = - (\bar{s}_2 - s_1) (B'_2 - iC'_2) \frac{L_2}{2} (\bar{b}_2) e^{2i(\beta_1 + \beta_2)} \frac{1}{\zeta_1^2}$$

$$N'^*_{\psi 9} = \left[\left[\frac{(a_{42})}{(\zeta_1 - C_1)^2} \right] + (B'_2 + iC'_2) \frac{L_2}{2} \left(\frac{(-a_2)}{(\zeta_1 - C_1)^2} + (b_2) e^{-2i(\beta_1 + \beta_2)} \right) \right]$$

$$N'^*_{\psi 10} = \left[-2\bar{C}_1 \left[\frac{(a_{32})}{(\zeta_1 - C_1)^3 e^{-2i(\beta_1 + \beta_2)}} \right] - 2\bar{C}_1 B_2 \frac{L_2}{2} \left(\frac{(a_1)}{(\zeta_1 - C_1)^3 e^{-2i(\beta_1 + \beta_2)}} \right) \right]$$

$$M'^*_{1} = \left(\frac{1}{(1 - \zeta_1 \bar{C}_1)^2} \right)$$

$$M'^*_{2} = \left(\frac{2\zeta_1}{(1 - \zeta_1 \bar{C}_1)^3} \right)$$

4.4.5 Stress Intensity Factor

The mode I and mode II stress intensity factors for the crack tips are obtained by using following formula given by Sih and Liebowitz[20],

$$K_I + \frac{K_{II}}{s_2} = 2\sqrt{\frac{\pi}{L}} \left(\frac{s_2 - s_1}{s_2} \right) \phi'(\zeta)$$

$$K_I + \frac{K_{II}}{s_1} = 2\sqrt{\frac{\pi}{L}} \left(\frac{s_1 - s_2}{s_1} \right) \psi'(\zeta)$$

Chapter 5

Results And Discussion

5.1 Preliminary Remarks

The stress analysis of infinite plate with openings is interesting field of investigation. It is expected that the general solutions will be useful to study the effect of type of loading, fiber orientation, laminate geometry and stacking sequence, etc. for crack approaching circular hole under inplane loading. In the present work, results are obtained for stress field around circular hole, elliptical hole and stress intensity factor at crack tip. The generalized solutions for stress functions obtained in previous chapter are coded using MATLAB 7.6 and also obtain the effect of center distance between crack and hole.

5.2 Methodology to Obtain Stress Field

The step wise procedure for numerical solution is as follows:

- a. Choose the value of biaxial load factor λ and loading angle β for the type of Loading.
- b. Calculate the value of compliance coefficient a_{ij} from their respective equations given in appendix A.

- c. Calculate the values of complex parameters of anisotropy s_1 and s_2 . Some of the values of these constants are shown in Table II.
- d. Calculate the values of $a_1, a_2, b_1, b_2, B, B', C', K_1, K_2, K_3, K_4$.
- e. Evaluate the derivatives of the second stage stress functions.
- f. Evaluate the value of stresses.
- g. Evaluate the value of stress intensity factor.

The following load cases are considered for the plate with various hole geometries.

- a. Uniaxial loading at infinity ($\lambda=0, \beta = 0$).
- b. Biaxial loading at infinity ($\lambda=1, \beta = 0$).
- c. Shear loading at infinity ($\lambda=-1, \beta = 45$).

The material properties used for numerical solution are as below:

Table I: Material Properties for different materials use for numerical solution

Material	E_1 (GPa)	E_2 (GPa)	G_{12} (GPa)	ν_{12}
Isotropic steel	207	207	79.6	0.3
E Glass/Epoxy	41	10.4	4.3	0.28
T300/5208 Graphite/Epoxy	181	10.3	7.17	0.28

Table II: Complex parameter of anisotropy

Sr. No.	Fiber Orientation Angle	Graphie/epoxy	Eglass/epoxy
		$E_1=181$ GPa, $E_2=10.30$ GPa, $G_{12} = 7.17$ GPa, $\nu_{12} = 0.28$, $\nu_{21} = 0.016$	$E_1=41$ GPa, $E_2=10.40$ GPa, $G_{12} = 4.30$ GPa, $\nu_{12} = 0.28$, $\nu_{21} = 0.07$
1	0°	$s_1 = 4.8936i$ $s_2 = 0.8566i$	$s_1 = 2.9194i$ $s_2 = 0.6801i$
2	15°	$s_1 = -2.2611 + 1.9288i$ $s_2 = 0.0678 + 0.8722i$	$s_1 = -1.2506 + 1.9412i$ $s_2 = 0.1394 + 0.7055i$
3	30°	$s_1 = -1.4750 + 0.7264i$ $s_2 = 0.1235 + 0.9177i$	$s_1 = -1.4334 + 0.7749i$ $s_2 = 0.0582 + 0.9640i$
4	45°	$s_1 = 0.1535 + 0.9881i$ $s_2 = -0.9198 + 0.3923i$	$s_1 = 0.3675 + 0.9300i$ $s_2 = -0.7900 + 0.6131i$
5	60°	$s_1 = 0.1440 + 1.0703i$ $s_2 = -0.5456 + 0.2687i$	$s_1 = 0.3899 + 1.1394i$ $s_2 = -0.4904 + 0.4395i$
6	75°	$s_1 = 0.0885 + 1.1397i$ $s_2 = -0.2560 + 0.2184i$	$s_1 = 0.2695 + 1.3642i$ $s_2 = -0.2345 + 0.3641i$
7	90°	$s_1 = 1.1674i$ $s_2 = 0.2043i$	$s_1 = 1.4704i$ $s_2 = 0.3425i$
8	$(\pm 45^\circ)_s$	$s_1 = 0.8597 + 0.5109i$ $s_2 = -0.8597 + 0.5109i$	$s_1 = -0.6978 + 0.7163i$ $s_2 = 0.6978 + 0.7163i$
9	$(0^\circ/90^\circ)_s$	$s_1 = 3.6403i$ $s_2 = 0.2747i$	$s_1 = 2.3704i$ $s_2 = 0.4219i$

5.3 Single Hole Problem

The problems of single hole is solved for infinite plate with circular and elliptical hole of E Glass/Epoxy [0/90]s subjected to uniaxial loading, biaxial loading and pure shear at infinity. (Refer Figure 5.1 to 5.20).

5.3.1 Stress Analysis of Isotropic Infinite Plate with Circular Hole

The problem of isotropic plate with circular hole is studied and the distribution of normalized tangential stresses σ_θ/σ for uniaxial loading, biaxial loading and for pure shear is obtained.

Uniaxial Loading ($\lambda=0, \beta=0$)

In this case, the maximum value of normalized tangential stress σ_θ/σ is 3.00 at $\theta=0^\circ, 180^\circ$ and the minimum value is -1.00 at $\theta=90^\circ, 270^\circ$ as shown in Figure [5.1]. The results are given in Table III. From table, the tangential stress is tensile around the hole at $\theta=0^\circ$ to $60^\circ, 200^\circ$ to 240° and at 301° to 360° and compressive at the remaining angles.

Biaxial Loading ($\lambda=1, \beta=0$)

In this case, the maximum value of normalized tangential stress σ_θ/σ is 2.00 at $\theta=0^\circ, 360^\circ$ as shown in Figure [5.2]. The results are given in Table III. There is no compressive stress developed around plate when it is subjected to Biaxial loading.

Pure Shear Loading ($\lambda=-1, \beta=45$)

In this case, the maximum value of normalized tangential stress σ_θ/σ is 4.00 at $\theta=45^\circ, 225^\circ$ and the minimum value is -4.00 at $\theta=135^\circ, 315^\circ$ as shown in Figure [5.3]. The results are given in Table III. From table, the tangential stress is tensile around hole at $\theta=0^\circ$ to $90^\circ, 181^\circ$ to 270° and compressive at the remaining angles.

The stress distribution for different loading condition are obtained and the values of normalized tangential stresses σ_θ/σ are tabulated in Table III.

Table III: Normalized Stress for different loading condition for isotropic Material plate with Circular Hole

Loading Condition	Normalized Tangential Stress					
	$(\sigma_\theta/\sigma)_{max}$		$(\sigma_\theta/\sigma)_{min}$		(σ_θ/σ)	
	Value	Degree	Value	Degree	Value	Degree
$\lambda = 0, \beta = 0$	3.00	$0^\circ, 180^\circ, 360^\circ$	-1	$90^\circ, 279^\circ$	0	$60^\circ, 120^\circ, 240^\circ, 300^\circ$
$\lambda = 1, \beta = 0$	2.00	0° to 360°	2	0° to 360°	0	-
$\lambda = -1, \beta = 45$	4	$45^\circ, 225^\circ$	-4	$135^\circ, 315^\circ$	0	$0^\circ, 90^\circ, 180^\circ, 270^\circ, 360^\circ$

Uniaxial Loading ($\lambda=0, \beta = 0$)

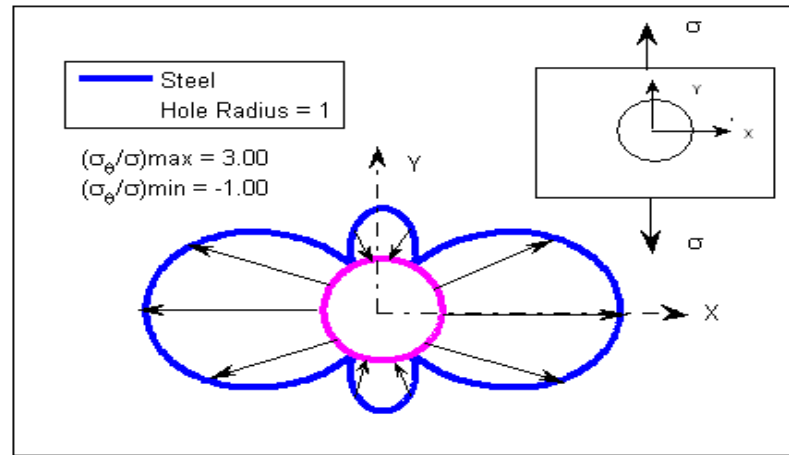


Figure 5.1: Tangential Stress σ_θ/σ for isotropic material($\lambda=0$ for $\beta = 0$ and $\alpha = 0$)

Biaxial Loading ($\lambda=1, \beta = 0$)

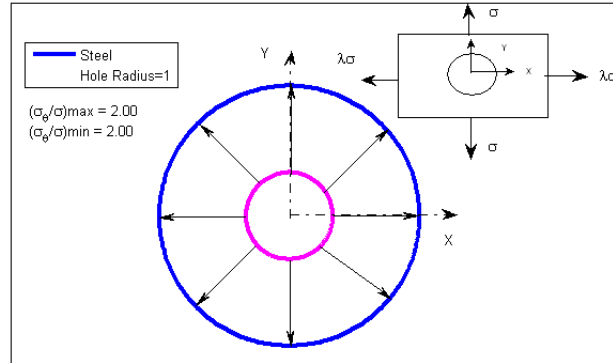


Figure 5.2: Tangential Stress σ_θ/σ for isotropic material($\lambda=1$ for $\beta = 0$ and $\alpha = 0$)

Pure Shear Loading ($\lambda=-1, \beta = 45$)

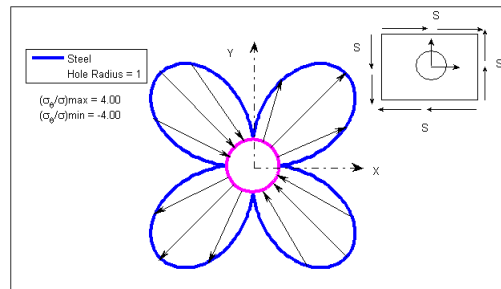


Figure 5.3: Tangential Stress σ_θ/σ for isotropic material($\lambda = -1$ for $\beta = 45$ and $\alpha = 0$)

5.3.2 Stress Analysis of Anisotropic Infinite Plate with circular Hole

The problem of single Circular hole is solved for infinite plate of E Glass/Epoxy $(0^\circ/90^\circ)_s$ subjected to uniaxial loading, bi-axial and pure shear loading at infinity with the material properties as shown in Table II. The complex parameter $s_1 = 2.3704i, s_2 = 0.4219i$ are taken.

Uniaxial Loading ($\lambda=0, \beta = 0$)

In this case, the maximum value of normalized tangential stress σ_θ/σ is 3.7916 at $\theta=0^\circ, 180^\circ$ and the minimum value is -1.00 at $\theta=90^\circ, 270^\circ$ as shown in Figure [5.4]. The results are given in Table IV. From table, the tangential stress is tensile around the hole at $\theta=0^\circ$ to $65^\circ, 115^\circ$ to 245° and at 295° to 360° and compressive at the remaining angles.

Biaxial Loading ($\lambda=1, \beta = 0$) In this, the maximum value of normalized tangential stress σ_θ/σ is 2.7916 at $\theta=0^\circ, 90^\circ$, and at $180^\circ, 270^\circ$ and the minimum value of normalized stress is 1.4329 at $\theta=45^\circ, 135^\circ$, and at $225^\circ, 315^\circ$ as shown in Figure [5.5]. The results are given in Table IV. There is no compressive stress developed around plate when it is subjected to Biaxial loading.

Pure Shear Loading ($\lambda = -1 \beta = 45$) In this the maximum value of normalized tangential stress σ_θ/σ is 3.4329 at $\theta=18^\circ, 72^\circ$, and at $198^\circ, 252^\circ$ and the minimum value is -3.4329 at $\theta=108^\circ, 162^\circ, 288^\circ, 342^\circ$ as shown in Figure [5.6]. The results are given in Table IV. From table, the tangential stress is tensile around hole at $\theta=0^\circ$ to $90^\circ, 181^\circ$ to 270° and compressive at the remaining angles.

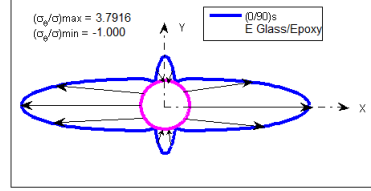
Uniaxial Loading ($\lambda=0, \beta = 0$)

Figure 5.4: Tangential Stress σ_θ/σ for E-Glass/Epoxy(0/90)_s ($\lambda=0, \beta = 0, \alpha = (0^\circ/90^\circ)_s$)

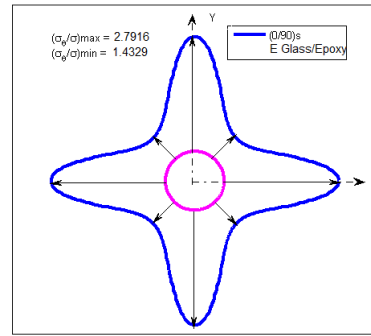
Biaxial Loading ($\lambda=1$)

Figure 5.5: Tangential Stress σ_θ/σ for E-Glass/Epoxy(0/90)_s ($\lambda=1, \beta = 0, \alpha = (0^\circ/90^\circ)_s$)

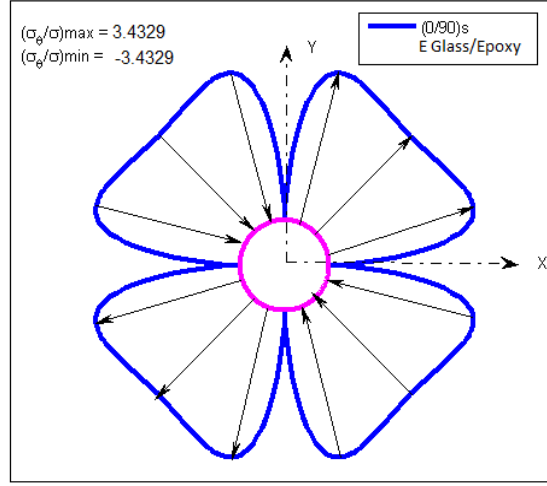
Pure Shear Loading ($\lambda = -1$ $\beta = 45$)

Figure 5.6: Tangential Stress σ_θ/σ for E-Glass/Epoxy(0/90)_s($\lambda = -1$ $\beta = 45$ $\alpha = (0^\circ/90^\circ)_s$)

The stress distribution for different loading condition are obtained and the values of normalized tangential stresses σ_θ/σ are tabulated in Table IV.

Table IV: Normalized Stress for different loading condition for Anisotropic Material plate with Circular Hole

Loading Condition	Normalized Tangential Stress					
	$(\sigma_\theta/\sigma)_{max}$		$(\sigma_\theta/\sigma)_{min}$		(σ_θ/σ)	
	Value	Degree	Value	Degree	Value	Degree
$\lambda = 0, \beta = 0$	3.7916	$0^\circ, 180^\circ, 360^\circ$	-1	$90^\circ, 270^\circ$	0	-
$\lambda = 1, \beta = 0$	2.7916	$0^\circ, 90^\circ, 180^\circ$ $270^\circ, 360^\circ$	1.4329	$45^\circ, 135^\circ$ $225^\circ, 315^\circ$	0	-
$\lambda = -1, \beta = 45$	3.4329	$18^\circ, 72^\circ$ $198^\circ, 252^\circ$	-3.4329	$108^\circ, 162^\circ$ $288^\circ, 342^\circ$	0	$0^\circ, 90^\circ, 180^\circ$ $270^\circ, 360^\circ$

5.3.3 Stress Analysis of Isotropic plate with circular hole using ANSYS

The solution of normalized tangential stress σ_θ/σ is obtained by using ANSYS 11 for isotropic plate with circular hole subjected to uniaxial and biaxial loading. The results are as shown in Figure [5.7] and [5.8]. Results are compared with results obtained from the ANSYS 11 and the results from the present method are close agreement with ANSYS's results. The comparison is as shown in Table V.

Uniaxial Loading($\lambda=1, \beta=0$)

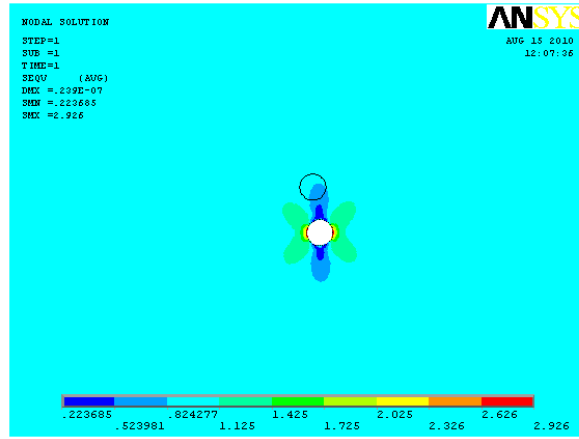


Figure 5.7: Stress σ_y for isotropic material($\lambda=0$ for $\beta = 0$)

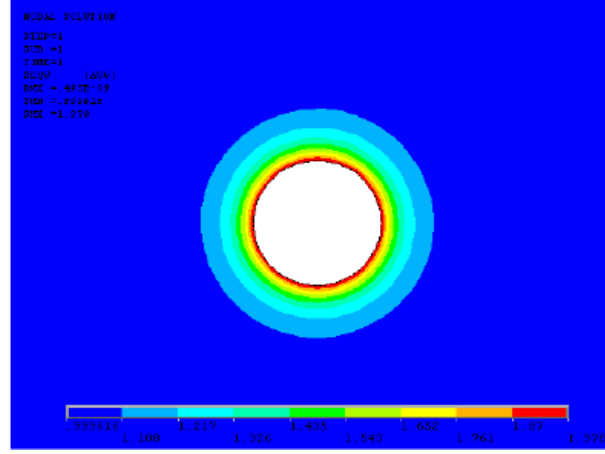
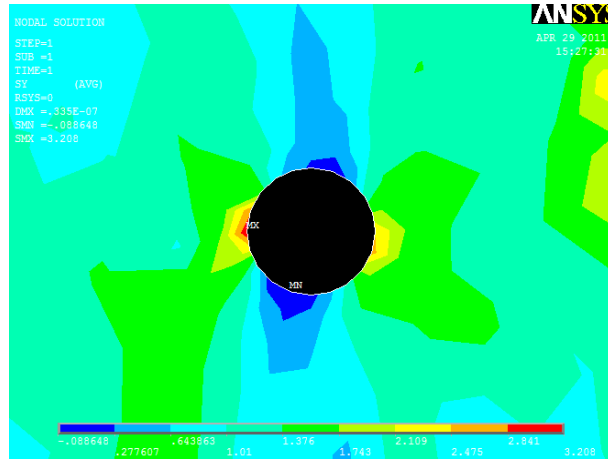
Biaxial Loading($\lambda=1, \beta=0$)Figure 5.8: Stress σ_y for isotropic material($\lambda=1$)

Table V: Comparison of results with results from ANSYS 11 for isotropic plate with circular hole

Loading condition	Maximum Normalized Tangential Stress $(\sigma_\theta/\sigma)_{max}$		
	(Present Method)	ANSYS result	Difference in percentage
Uniaxial	3.00	2.992	0.0027
Biaxial	2.00	1.97	-0.03
Pure Shear	2.00	-	-

5.3.4 Stress Analysis of Anisotropic plate with circular hole using ANSYS

The solution of normalized tangential stress σ_θ/σ is obtained by using ANSYS 11 for anisotropic plate with elliptical hole subjected to uniaxial and biaxial loading. The results are as shown in Figure [5.9] and [5.10]. The results obtained from the ANSYS 11 and the results from the present method are close agreement with ANSYS's results. The comparison is as shown in Table VI. **Uniaxial Loading($\lambda=1, \beta=0$)**

Figure 5.9: Stress σ_y for E-Glass/Epoxy $(0/90)_s$ ($\lambda=0$ for $\beta = 0$)

Biaxial Loading($\lambda=1, \beta=0$)

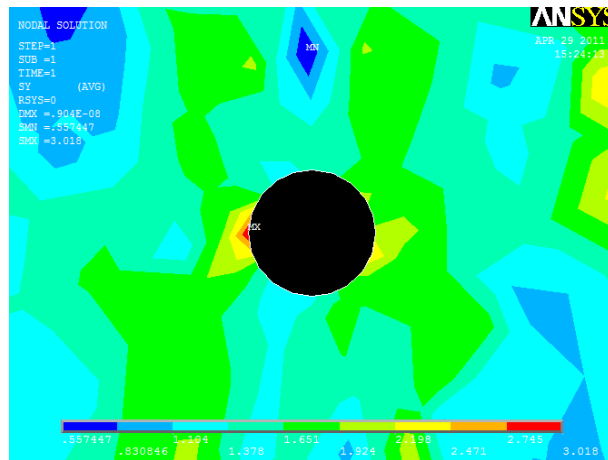
Figure 5.10: Stress σ_y for E-Glass/Epoxy $(0/90)_s$ ($\lambda=1$)

Table VI: Comparison of results with results from ANSYS 11 for anisotropic plate with circular hole

Loading condition	Maximum Normalized Tangential Stress $(\sigma_\theta/\sigma)_{max}$		
	Present method	ANSYS result	Difference
Uniaxial	3.7916	3.208	0.1819
Biaxial	2.7916	3.018	-0.0750
Pure Shear	3.4329	-	-

5.3.5 Stress Analysis of Isotropic Infinite Plate with Elliptic Hole

The problem of isotropic plate with elliptical hole is studied and the distribution of normalized tangential stresses σ_θ/σ for uniaxial loading, biaxial loading and for pure shear is obtained. For elliptical hole, mapping function constant is $m=(a-b)/(a+b)$. Where, a and b is the semi major axis and semi minor axis. Elliptical hole considered here is having semi major axis of 1.3 units and semi minor axis of 0.7 units.

Uniaxial Loading ($\lambda=0, \beta=0$)

In this, the maximum value of normalized tangential stress σ_θ/σ is 4.7145 at $\theta=0^\circ, 180^\circ$ and the minimum value is -1.00 at $\theta=90^\circ, 270^\circ$ as shown in Figure [5.11]. The results are given in Table VII. From table, the tangential stress is tensile around the hole at $\theta=0^\circ$ to $49^\circ, 131^\circ$ to 229° and compressive at the remaining angles.

Biaxial Loading ($\lambda=1, \beta=0$)

In this, the maximum value of normalized tangential stress σ_θ/σ is 3.7145 at $\theta=0^\circ, 180^\circ$ as shown in Figure [5.12]. There is no compressive stress developed around plate when it is subjected to Biaxial loading.

Pure Shear Loading ($\lambda=-1, \beta=45$)

In this, the maximum value of normalized tangential stress σ_θ/σ is 4.038 at $\theta=27^\circ, 207^\circ$ and the minimum value is -4.038 at $\theta=153^\circ, 333^\circ$ as shown in Figure [5.13]. The results are given in Table VII.

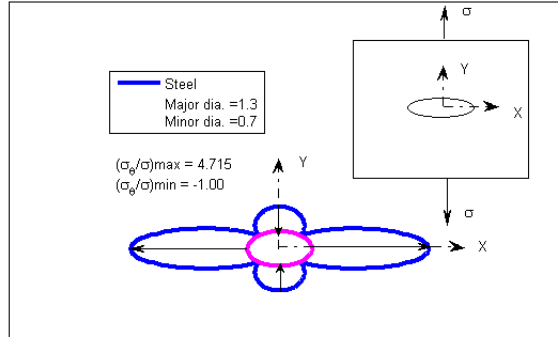
Uniaxial Loading ($\lambda=0, \beta=0$)

Figure 5.11: Tangential Stress σ_θ/σ for isotropic material ($\lambda=0$ for $\beta=0$ and $\alpha=0$)

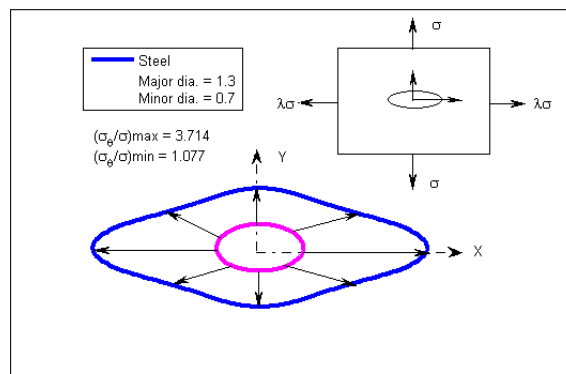
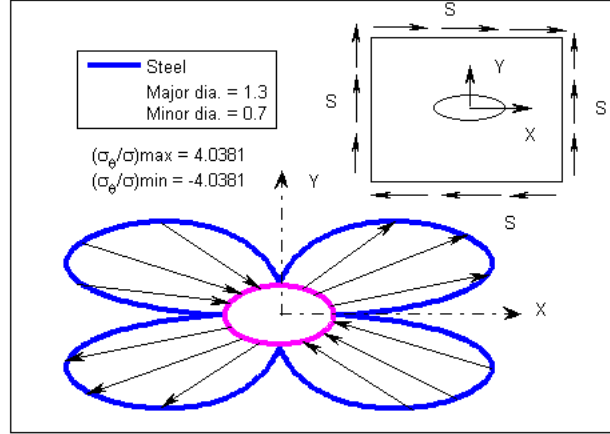
Biaxial Loading ($\lambda=1, \beta=0$)

Figure 5.12: Tangential Stress σ_θ/σ for isotropic material ($\lambda=1$ for $\beta=0$ and $\alpha=0$)

Pure Shear Loading ($\lambda=-1, \beta = 45$)Figure 5.13: Tangential Stress σ_θ/σ for isotropic material($\lambda = -1$ for $\beta = 45$)

The stress distribution for different loading condition are obtained and the values of normalized tangential stresses σ_θ/σ are tabulated in Table VII.

Table VII: Normalized Stress for different loading condition for Isotropic Material plate with Elliptical Hole

Loading Condition	Normalized Tangential Stress					
	$(\sigma_\theta/\sigma)_{max}$		$(\sigma_\theta/\sigma)_{min}$		(σ_θ/σ)	
	Value	Degree	Value	Degree	Value	Degree
$\lambda = 0, \beta = 0$	4.7145	$0^\circ, 180^\circ, 360^\circ$	-1	$90^\circ, 270^\circ$	0	-
$\lambda = 1, \beta = 0$	3.715	$0^\circ, 180^\circ, 360^\circ$	1.0770	$90^\circ, 270^\circ$	0	-
$\lambda = -1, \beta = 45$	4.0381	$27^\circ, 207^\circ$	-4.0381	$153^\circ, 333^\circ$	0	$0^\circ, 90^\circ, 180^\circ, 270^\circ, 360^\circ$

5.3.6 Stress Analysis of Anisotropic Plate with Elliptic Hole

The problem of single Elliptical hole is solved for infinite plate of E Glass/Epoxy $(0^\circ/90^\circ)_s$ subjected to uniaxial loading, bi-axial and pure shear loading at infinity with the material properties as shown in table I. The complex parameter $s_1 = 2.3704i, s_2 = 0.4219i$ are taken.

Uniaxial Loading ($\lambda=0, \beta = 0$)

In this, the maximum value of normalized tangential stress σ_θ/σ is 6.1844 at $\theta=0^\circ, 180^\circ$ and the minimum value is -0.0282 at $\theta=90^\circ, 270^\circ$ as shown in Figure [5.14]. The results are given in Table VIII. From table, the tangential stress is tensile around the hole at $\theta=0^\circ$ to $53^\circ, 128^\circ$ to 232° and at 308° to 360° .

Biaxial Loading ($\lambda=1, \beta = 0$)

In this, the maximum value of normalized tangential stress σ_θ/σ is 5.1844 at $\theta=0^\circ, 180^\circ$ and the minimum value of normalized tangential stress is 1.2834 at $\theta=40^\circ, 140^\circ, 220^\circ, 320^\circ$ as shown in Figure [5.15]. The results are given in Table VIII. There is no compressive stress developed around plate when it is subjected to Biaxial loading.

Pure Shear Loading ($\lambda = -1 \beta = 45$)

In this, the maximum value of normalized tangential stress σ_θ/σ is 3.4876 at $\theta=10^\circ, 190^\circ$ and the minimum value is -3.4876 at $\theta=170^\circ, 350^\circ$ as shown in Figure [5.16]. The results are given in Table VIII. From table, the tangential stress is tensile around hole at $\theta=0^\circ$ to $90^\circ, 181^\circ$ to 270° and compressive at the remaining angles.

The stress distribution for different loading condition are obtained and the values of normalized tangential stresses σ_θ/σ are tabulated in Table VIII.

Table VIII: Normalized Stress for different loading condition for Anisotropic Material Plate with Elliptical Hole

Loading Condition	Normalized Tangential Stress					
	$(\sigma_\theta/\sigma)_{max}$		$(\sigma_\theta/\sigma)_{min}$		(σ_θ/σ)	
	Value	Degree	Value	Degree	Value	Degree
$\lambda = 0, \beta = 0$	8.2708	$0^\circ, 180^\circ, 360^\circ$	-1	$90^\circ, 270^\circ$	0	-
$\lambda = 1, \beta = 0$	7.2708	$0^\circ, 180^\circ, 360^\circ$	0.9861	$40^\circ, 140^\circ, 220^\circ, 320^\circ$	0	-
$\lambda = -1, \beta = 45$	3.5969	$10^\circ, 190^\circ$	-3.5969	$170^\circ, 350^\circ$	0	$0^\circ, 90^\circ, 180^\circ$

Uniaxial Loading ($\lambda=0, \beta = 0$)

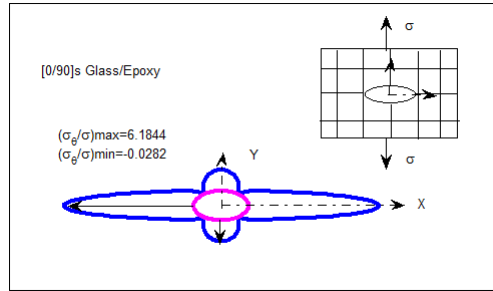
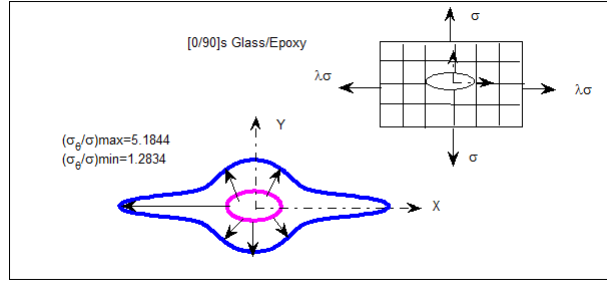
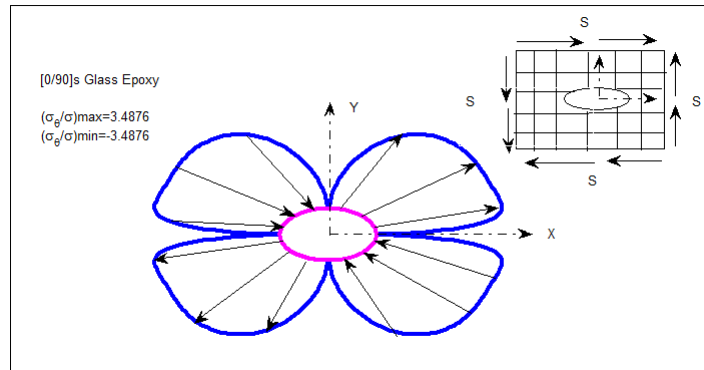


Figure 5.14: Tangential Stress σ_θ/σ for E-Glass/Epoxy $(0/90)_s$ ($\lambda=0, \beta = 0, \alpha = (0^\circ/90^\circ)_s$)

Biaxial Loading ($\lambda=1$)Figure 5.15: Tangential Stress σ_θ/σ for E-Glass/Epoxy $(0/90)_s$ ($\lambda=1$, $\alpha = (0^\circ/90^\circ)_s$)**Pure Shear Loading ($\lambda = -1$ $\beta = 45^\circ$)**Figure 5.16: Tangential Stress σ_θ for E-Glass/Epoxy $(0/90)_s$ ($\lambda = -1$ $\beta = 45^\circ$ $\alpha = (0^\circ/90^\circ)_s$)

5.3.7 Stress Analysis of Isotropic plate with elliptical hole using ANSYS

The solution of normalized tangential stress σ_θ/σ is obtained by using ANSYS 11 for isotropic plate with elliptical hole subjected to uniaxial and biaxial loading. The results are as shown in Figure [5.17] and [5.18]. The results obtained from the ANSYS 11 and the results from the present method are close agreement with ANSYS's results. The comparison is as shown in Table IX.

Uniaxial Loading($\lambda=1, \beta=0$)

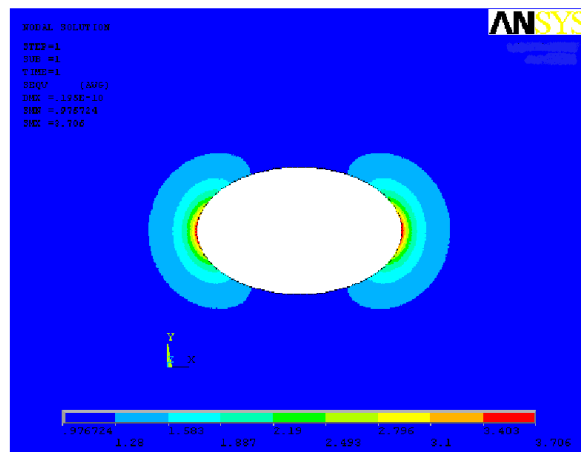


Figure 5.17: Stress σ_y for isotropic material ($\lambda=0$ for $\beta = 0$)

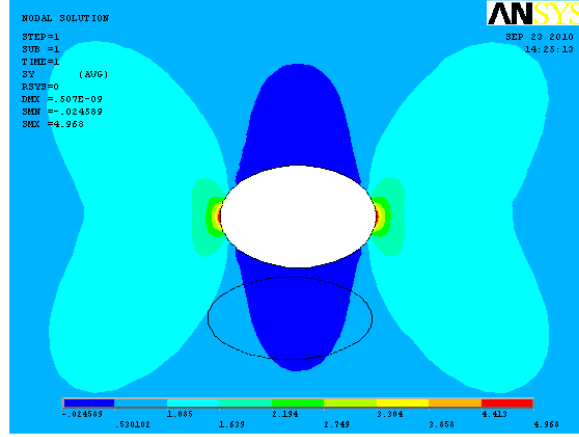
Biaxial Loading($\lambda=1, \beta=0$)Figure 5.18: Stress σ_y for isotropic material($\lambda=1$)

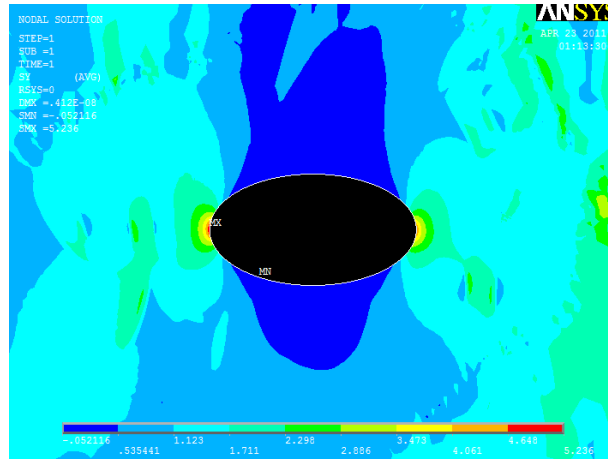
Table IX: Comparison of results with results from ANSYS 11 for isotropic plate with elliptical hole

Loading condition	Maximum Normalized Tangential Stress $(\sigma_\theta/\sigma)_{max}$		
	Present method	ANSYS result	Difference
Uniaxial	4.7	4.968	-0.0570
Biaxial	3.714	3.70	0.006
Pure Shear	4.038	-	-

5.3.8 Stress Analysis of Anisotropic plate with elliptical hole using ANSYS

The solution of normalized tangential stress σ_θ/σ is obtained by using ANSYS 11 for anisotropic plate with elliptical hole subjected to uniaxial and biaxial loading. The results are as shown in Figure [5.19] and [5.20]. The results obtained from the ANSYS 11 and the results from the present method are close agreement with ANSYS's results. The comparison is as shown in Table X.

Uniaxial Loading($\lambda=1, \beta=0$)

Figure 5.19: Stress σ_y for E-Glass/Epoxy $(0/90)_s$ ($\lambda=0$ for $\beta = 0$)

Biaxial Loading($\lambda=1, \beta=0$)

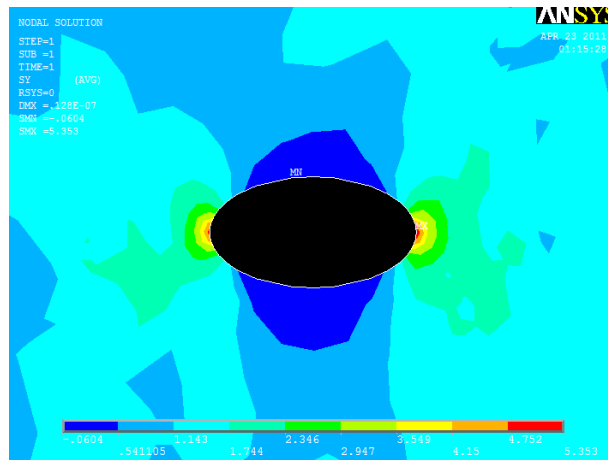
Figure 5.20: Stress σ_y for E-Glass/Epoxy $(0/90)_s$ ($\lambda=1$)

Table X: Comparison of results with results from ANSYS 11 for anisotropic plate with elliptical hole

Loading condition	Maximum Normalized Tangential Stress $(\sigma_\theta/\sigma)_{max}$		
	Present method	ANSYS result	Difference
Uniaxial	6.1844	5.353	0.1533
Biaxial	5.1844	5.236	-0.0099
Pure Shear	3.4876	-	-

5.4 Stress Analysis of Infinite Orthotropic plate with Crack

Using generalized stress functions, stress intensity factors for different loading conditions and crack orientations can be obtained. Also, the stress field around the cracks can be found. In this study, stress intensity factors are normalized with those for the case of a central crack of length $2a$ in an infinite plate. The crack orientation angle is varied from 0° to 90° and for different values of loading factor, the values of K_I/K_0 and K_{II}/K_0 are obtained.

For Graphite/Epoxy (0/90) values of K_I/K_0 and K_{II}/K_0 can be seen from Figure [5.21]. For uniaxial loading ($\lambda = 0$), the K_I/K_0 is unity at crack orientation angle $\alpha = 0$, and then it reduces monotonically to zero. The K_{II}/K_0 for uniaxial loading reduces up to 45° and then increases to zero. For biaxial loading ($\lambda = 1$), K_I/K_0 and K_{II}/K_0 are found 1.0 and 0 respectively for all orientations of crack.

The Figure [5.22] shows variation in K_I/K_0 and K_{II}/K_0 for Graphite/Epoxy (0/90) under shear loading at infinity.

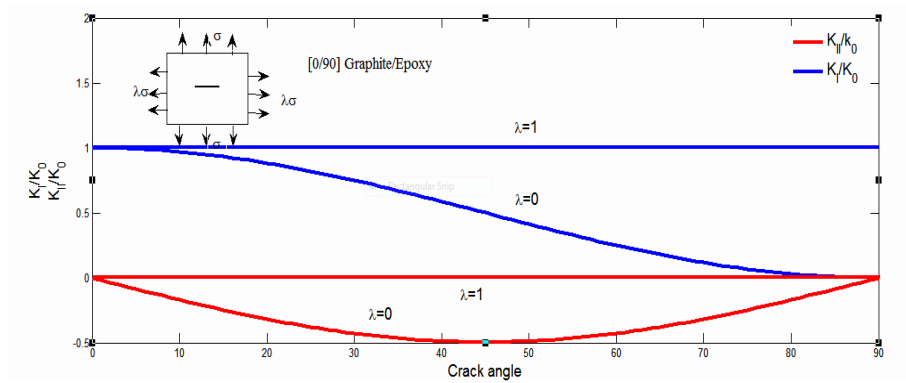


Figure 5.21: Change in K_I/K_0 and K_{II}/K_0 with crack angle for Graphite/Epoxy (0/90)

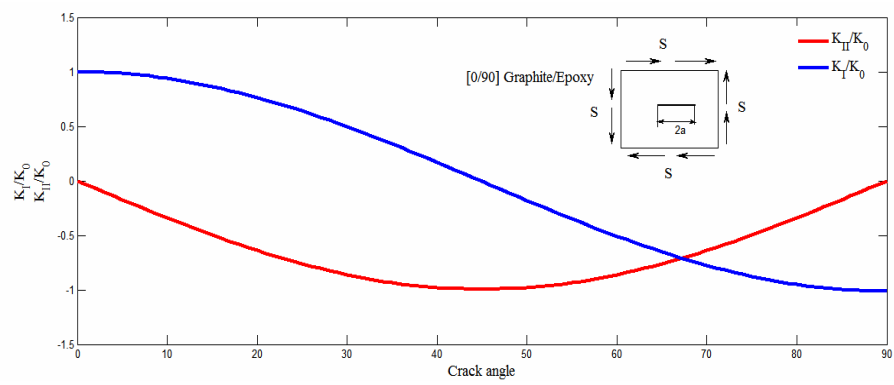


Figure 5.22: Change in K_I/K_0 and K_{II}/K_0 with crack angle for Graphite/Epoxy (0/90) under shear load at infinity

5.5 Crack Approaching Circular Hole Problem

The problem of crack approaching circular hole is solved for E Glass/Epoxy in $[0_n/90_m]_s$ laminate as shown in Figure [3.6]. The results are obtained for stress field around crack approaching circular hole in $[0_n/90_m]_s$ laminates.

5.5.1 Effect of Center Distance on Hole

The effect of center distance between crack and hole on stresses under different loading conditions are studied for E-Glass/Epoxy. The distribution of stresses due to uniaxial loading and equi-biaxial loading on E-Glass/Epoxy $[0/90]_s$ laminates are shown in Figure [5.23] to [5.28] when center distance between crack and hole is 5 units.

Figure [5.23] and Figure [5.24] shows that the maximum and minimum value of stresses in Y-direction for uniaxial loading and equi-biaxial loading respectively. Maximum and minimum value of stresses for uniaxial loading are 3.2427 and -1.8620 respectively. For equi-biaxial loading, maximum and minimum value of stresses are 2.4706 and 0.00.

Figure [5.25] and Figure [5.26] shows the maximum and minimum value of tangential stresses for uniaxial and equi-biaxial loading respectively. Maximum and minimum value of tangential stresses for uniaxial loading are 3.2427 and -1.8620 respectively. For equi-biaxial loading, maximum and minimum value of tangential stresses are 2.5110 and 1.6426. There is no compressive stress developed around hole when it is subjected to equi-biaxial loading.

Figure [5.27] and Figure [5.28] show the interaction effect on hole for distance between crack and hole is 5 and 3.5 units, respectively. The points on the hole circumference facing crack geometry shows more interaction. The comparison with single hole result is also evident from the Figure [5.27] and Figure [5.28].

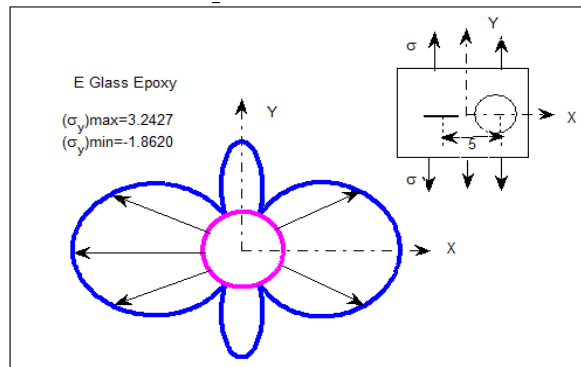


Figure 5.23: Stress in Y-direction (σ_y) when plate is subjected to uniaxial loading ($\lambda = 0$) (E-Glass/Epoxy $[0/90]_s$)

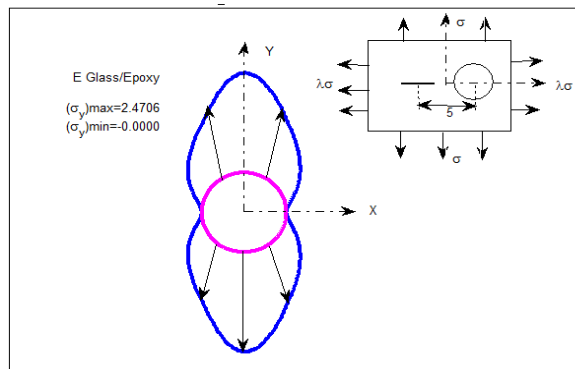


Figure 5.24: Stress in Y-direction (σ_y) when plate is subjected to equi-biaxial loading ($\lambda = 1$) (E-Glass/Epoxy $[0/90]_s$)

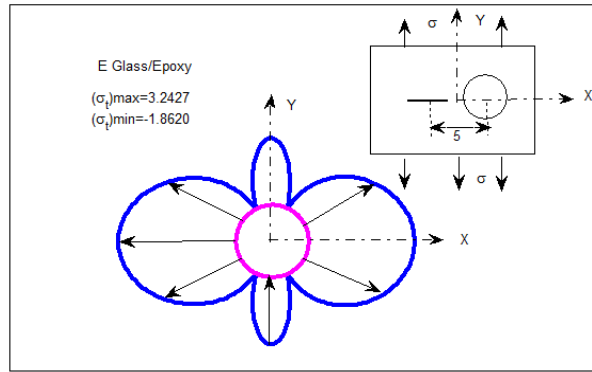


Figure 5.25: Tangential Stress (σ_t) when plate is subjected to uniaxial loading ($\lambda = 0$) (E-Glass/Epoxy $[0/90]_s$)

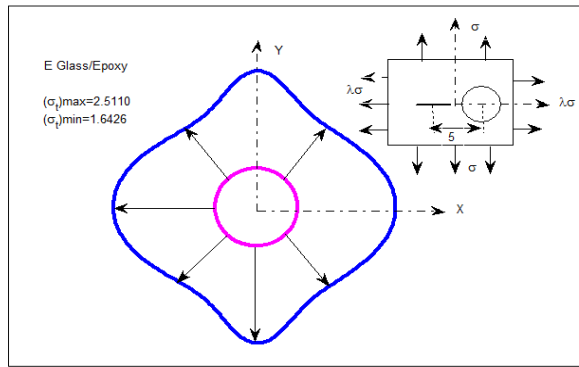


Figure 5.26: Tangential Stress (σ_t) when plate is subjected to equi-biaxial loading ($\lambda = 1$) (E-Glass/Epoxy $[0/90]_s$)

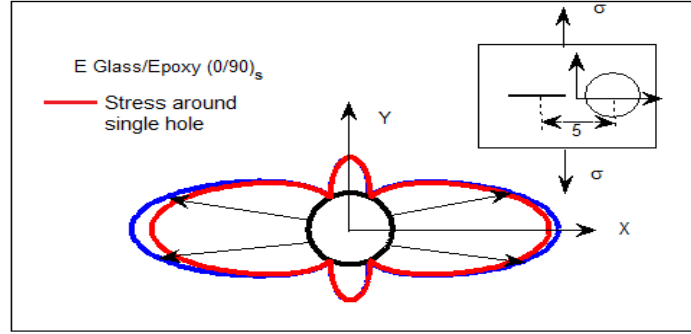


Figure 5.27: Interaction effect between crack and hole ($C_0 = 5$) (E-Glass/Epoxy $[0/90]_s$)

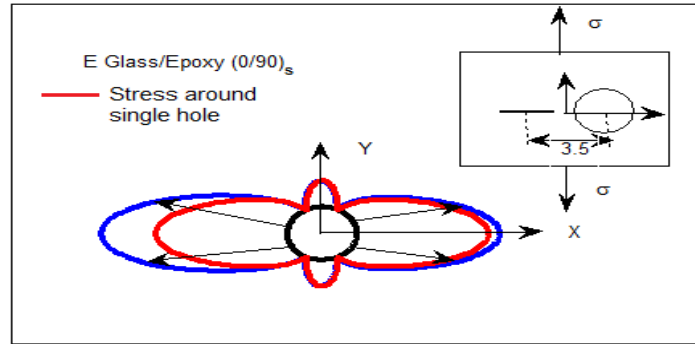


Figure 5.28: Interaction effect between crack and hole ($C_0 = 3.5$) (E-Glass/Epoxy $[0/90]_s$)

Various graphs are plotted for center distance between crack and hole, for different crack length and corresponding values of stresses (Refer Figure [5.29] to [5.30]). Figure [5.29] shows the effect of center distance on hole for uniaxial loading and equi-biaxial loading for E-Glass/Epoxy $[(0/90)_s]$ laminate where the crack length is 4. Effect of center distance on hole for crack length of 6 is shown in Figure [5.30].

It is found that if the center distance between crack and hole is less the interaction effect is more and the stress values are increases. When two holes are far apart from each other the solution reduces to the single hole problem.

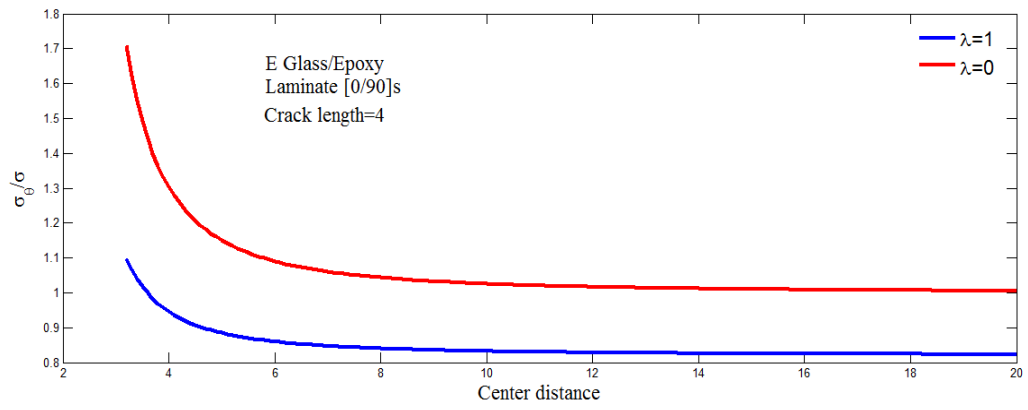


Figure 5.29: Effect of center distance on normalized tangential stress on hole for crack length 4 (E-Glass/Epoxy [0/90]_s)

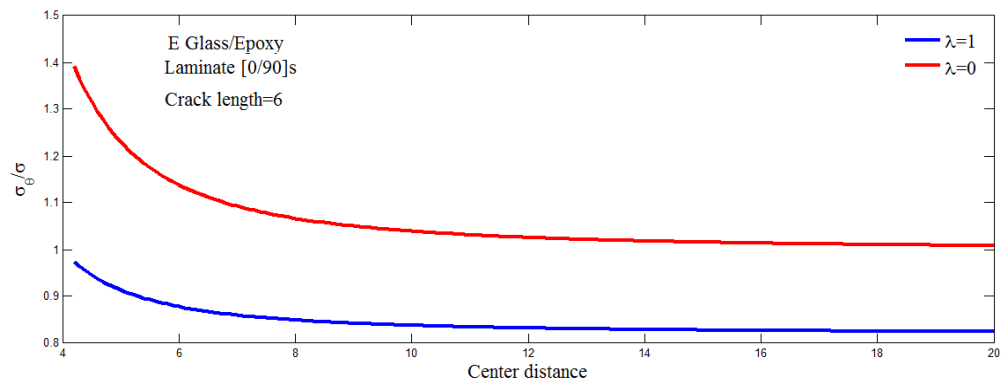


Figure 5.30: Effect of center distance on normalized tangential stress on hole for crack length 6 (E-Glass/Epoxy [0/90]_s)

5.5.2 Effect of Center Distance on Crack

The stress intensity factor obtained for a crack approaching circular hole for E-Glass/Epoxy in $[0_n/90_m]_s$ laminates. Since cross-ply laminated composite is used in the numerical calculation, only the mode I stress intensity factor existed. The stress intensity factors are presented as functions of the normalized crack length $a/(d-R)$ for cross-ply laminated composite. In this, stress intensity factors are normalized with those for the case of a central crack of length $2a$ in an infinite plate.

Figure [5.31], [5.32] and [5.33] show the normalized stress intensity factors for a crack approaching circular hole in $[0_n/90_m]_s$ laminates with $d/R=2,3$, and 4 respectively, under uniform tensile stress. The mode I stress intensity factors for the $[0_n/90_m]_s$ laminate exist between those for $\alpha = 0^\circ$ and those for $\alpha = 90^\circ$ in whole range of crack length and decrease as the percentage of 0° plies increases. In the range of large crack lengths the differences of the mode I stress intensity factors for the $[0_n/90_m]_s$ laminate become smaller as d/R increases.

Figure [5.34], [5.35] and [5.36] shows the normalized stress intensity factors for a crack approaching circular hole in $[0]$, $[0_2/90]_s$ and $[0/90]_s$ laminates under uniform tensile stress, respectively. The stress intensity factor becomes smaller as d/R increases and the differences of the mode I stress intensity factor for d/R become a little larger as the percentage of 90° plies increases.

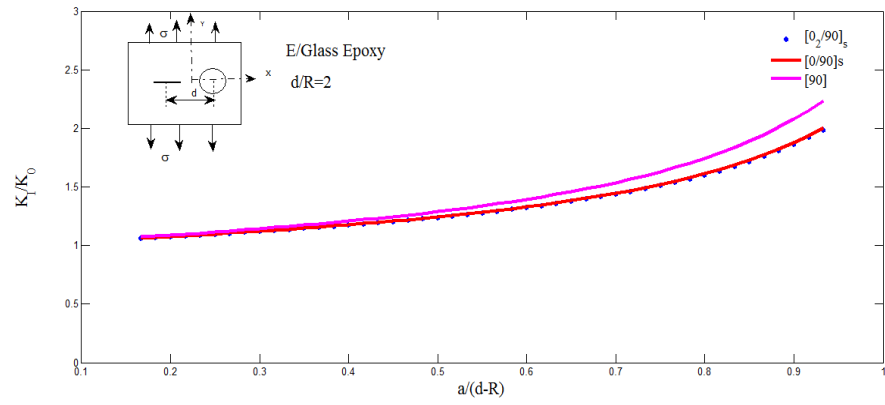


Figure 5.31: normalized stress intensity factors for a crack approaching circular hole in cross ply laminate $[0_n/90_m]_s$ under uniform tensile stress ($d/R = 2$)

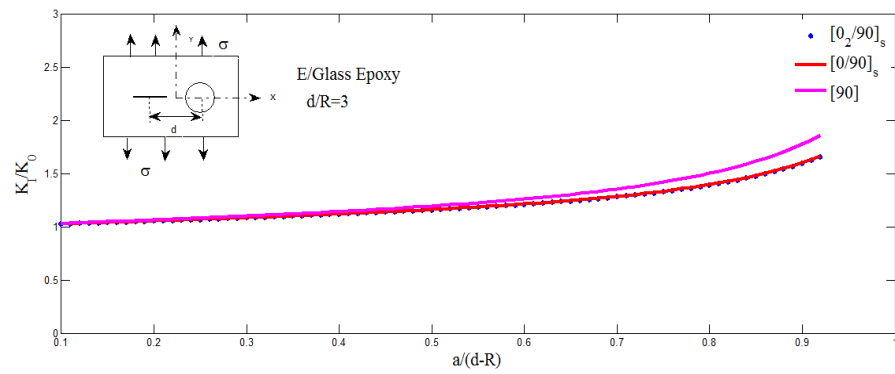


Figure 5.32: normalized stress intensity factors for a crack approaching circular hole in cross ply laminate $[0_n/90_m]_s$ under uniform tensile stress ($d/R = 3$)

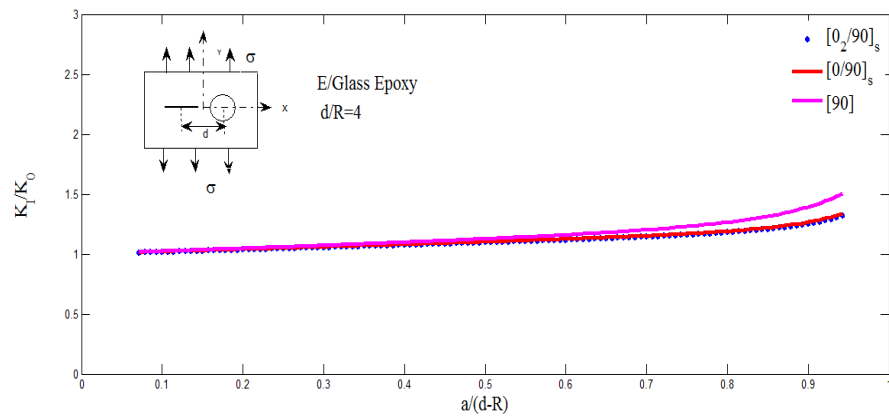


Figure 5.33: normalized stress intensity factors for a crack approaching circular hole in cross ply laminate $[0_n/90_m]_s$ under uniform tensile stress ($d/R = 4$)

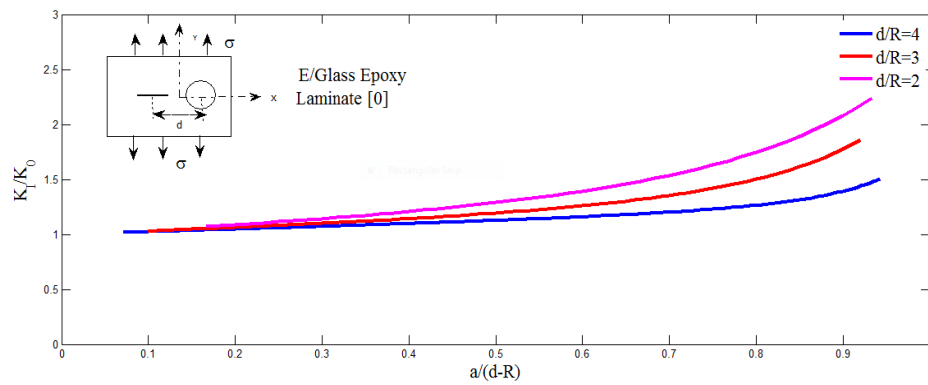


Figure 5.34: normalized stress intensity factors for a crack approaching circular hole in cross ply lamina $[0]$ under uniform tensile stress

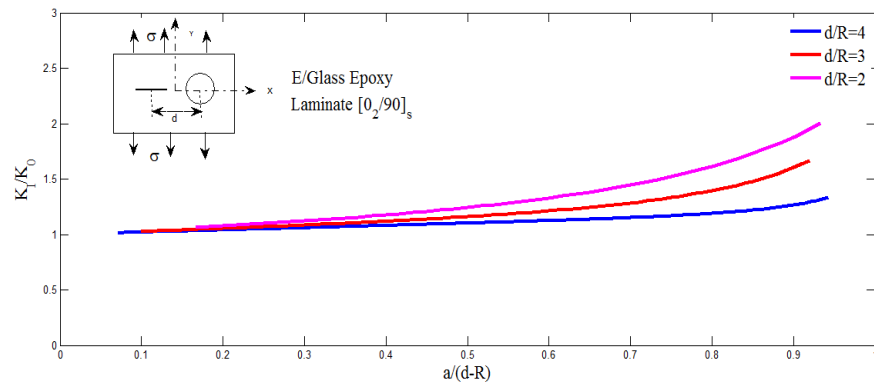


Figure 5.35: normalized stress intensity factors for a crack approaching circular hole in cross ply laminate $[0_2/90]_s$ under uniform tensile stress

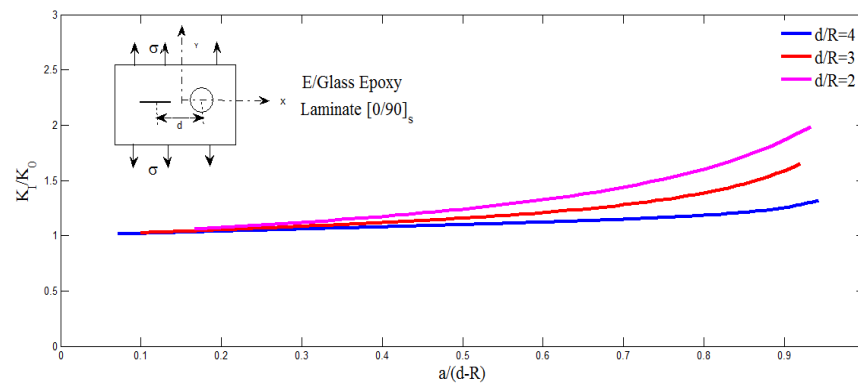


Figure 5.36: normalized stress intensity factors for a crack approaching circular hole in cross ply laminate $[0/90]_s$ under uniform tensile stress

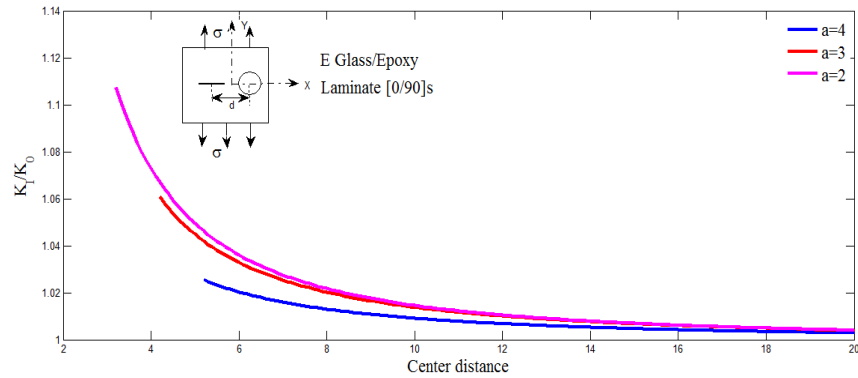


Figure 5.37: Effect of center distance on stress intensity factor at crack tip B in cross ply laminate $[0/90]_s$ under uniform tensile stress

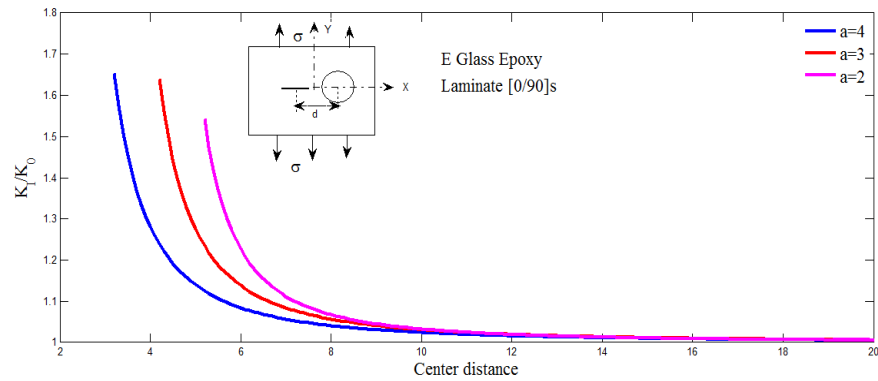


Figure 5.38: Effect of center distance on stress intensity factor at crack tip A in cross ply laminate $[0/90]_s$ under uniform tensile stress

Figure [5.37] and [5.38] shows the effect of center distance on stress intensity factor at crack tip B and at crack tip A, respectively. It shows that center distance between crack and hole are decrease, the interaction effect increases and as the center distance increases the interaction effect decreases and the solution tends to single crack solution.

5.6 Closing Remarks

In this chapter the solution of infinite orthotropic plate with crack approaching circular hole is obtained using Mushkhelishvili's complex variable formulation and Schwarz alternating method. The generalized formulation is coded in MATLAB 7.6 and few numerical results are obtained. The numerical results are employed to understand, effect of center distance between crack and hole on various stresses. The stress field for single hole problem is also obtained for few cases. Some of the problems are solved using ANSYS and results are compared with present method.

Chapter 6

Conclusion and Future Scope

6.1 Conclusion

The general solution presented here is extremely useful to study the interaction effect between the crack and hole under different loading condition. The conclusion for the present work is as follows:

- The fiber orientation angle has a significant effect on the stresses.
- The present method of solution helps to study the interaction effect of crack and hole under different loading conditions.
- When the crack and hole are far apart the solution reduces to single hole or single crack problem.
- The numerical solutions for E-Glass/Epoxy $[0_n/90_m]_s$ reveals that material of the plate and stacking sequence has significant effect on SIF.
- The present formulation is for orthotropic plate. The solution can be used for isotropic material by choosing suitable constants.

6.2 Contributions of the Present Work

- The Schwarz's alternating method is extended to analyze the interaction effect of crack and hole for infinite composite plate.
- The stress functions for single hole and crack approaching circular hole problem under different loading conditions are presented for infinite composite plate. These stress functions are handy tool for the designer to evaluate stresses around holes.

6.3 Limitations

- The solution presented considers two dimensional case only.
- The effect of transverse normal stress and strain and transverse shear strains are not considered.

6.4 Future Scope

- Stress analysis of infinite orthotropic plate with crack approaching two circular holes.
- Stress analysis of composite plate with multiple holes and crack.
- Stress analysis of a crack approaching a hole subjected to bending/twisting at infinity.
- Stress analysis of finite orthotropic plate with crack approaching circular hole.

Appendix A

Compliance Coefficients

Equations for calculating compliance coefficients for single layer and multilayered anisotropic plates are as given below.

A-Unidirectional layers with oriented fibers

For an orthotropic material, the compliance matrix components in terms of engineering constants are

$$S_{ij} = \begin{bmatrix} \frac{1}{E_1} & \frac{-v_{12}}{E_2} & \frac{-v_{31}}{E_3} & 0 & 0 & 0 \\ \frac{-v_{21}}{E_2} & \frac{1}{E_2} & \frac{-v_{32}}{E_3} & 0 & 0 & 0 \\ \frac{-v_{13}}{E_1} & \frac{-v_{23}}{E_2} & \frac{1}{E_3} & 0 & 0 & 0 \\ 0 & 0 & 0 & \frac{1}{G_{23}} & 0 & 0 \\ 0 & 0 & 0 & 0 & \frac{1}{G_{31}} & 0 \\ 0 & 0 & 0 & 0 & 0 & \frac{1}{G_{12}} \end{bmatrix} \quad (A.1)$$

The equation above can be reduced to

$$S_{ij} = \begin{bmatrix} \frac{1}{E_1} & \frac{-v_{21}}{E_2} & 0 \\ \frac{-v_{12}}{E_1} & \frac{1}{E_2} & 0 \\ 0 & 0 & \frac{1}{G_{12}} \end{bmatrix} \quad (A.2)$$

A unidirectional lamina is shown in Figure below. The transformed compliance coefficient a_{ij} are obtained by the following equations.

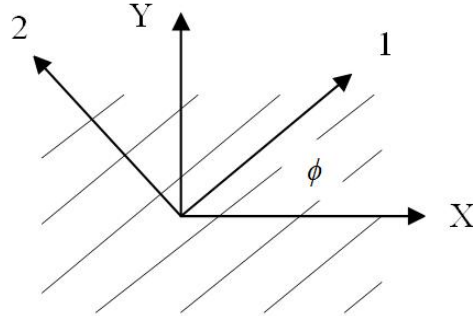


Figure A.1: Unidirectional Lamina

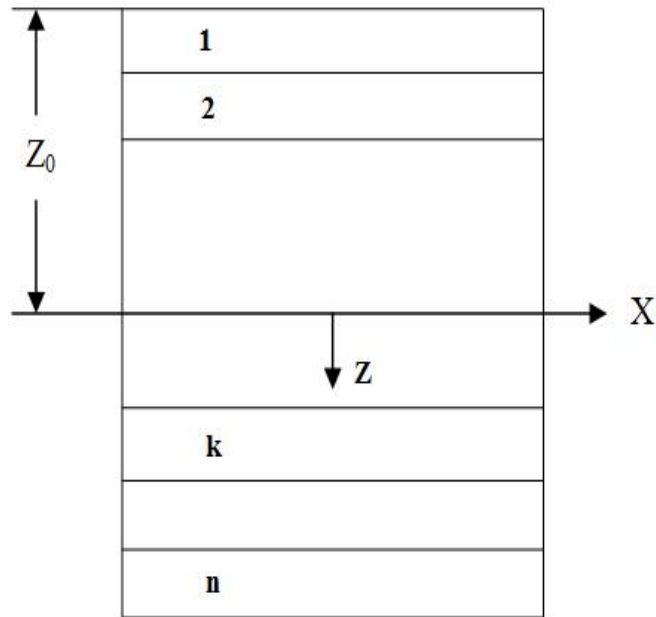


Figure A.2: Geometry of multilayered laminate

The transformed compliance coefficients a_{ij} are obtained by the following equations.

$$\begin{aligned}
a_{11} &= s_{11}m^4 + (2s_{12} + s_{66})m^2n^2 + s_{22}n^4 \\
a_{12} &= s_{12}(m^4 + n^4) + (s_{11} + s_{22} - s_{66})m^2n^2 \\
a_{22} &= s_{11}n^4 + (2s_{12} + s_{66})m^2n^2 + s_{22}m^4 \\
a_{16} &= (2s_{11} - 2s_{12} - s_{66})nm^3 - (2s_{22} - 2s_{12} - s_{66})mn^3 \\
a_{26} &= (2s_{11} - 2s_{12} - s_{66})n^3m - (2s_{22} - 2s_{12} - s_{66})m^3n \\
a_{66} &= 2(2s_{11} + 2s_{22} - 4s_{12} - s_{66})n^2m^2 + s_{66}(m^4 + n^4)
\end{aligned} \tag{A.3}$$

Where $m = \cos(\phi)$; $n = \sin(\phi)$, ϕ is the fiber orientation angle w.r.t. x-axis.

B- Multilayered plate

The stiffness coefficient along the principal material directions are written in term of engineering constants. They are as follows,

$$\begin{aligned}
Q_{11} &= \frac{E_1}{1 - \nu_{12} \nu_{21}} \\
Q_{22} &= \frac{E_2}{1 - \nu_{12} \nu_{21}} \\
Q_{12} &= \frac{\nu_{12} E_1}{1 - \nu_{12} \nu_{21}} \\
Q_{66} &= G_{12}
\end{aligned} \tag{A.4}$$

The transformed stiffness coefficients for unidirectional layers with oriented fibers are given by the following equations.

$$\begin{aligned}
\overline{Q_{11}} &= U_1 + U_2 \cos 2\phi + U_3 \cos 4\phi \\
\overline{Q_{12}} &= U_4 - U_3 \cos 4\phi \\
\overline{Q_{22}} &= U_1 - U_2 \cos 2\phi + U_3 \cos 4\phi \\
\overline{Q_{16}} &= \frac{1}{2} U_2 \sin 2\phi + U_3 \sin 4\phi \\
\overline{Q_{16}} &= \frac{1}{2} U_2 \sin 2\phi - U_3 \sin 4\phi \\
\overline{Q_{66}} &= U_5 - U_3 \cos 4\phi
\end{aligned} \tag{A.5}$$

Where

$$\begin{aligned}
U_1 &= \frac{3Q_{11} + 3Q_{22} + 2Q_{12} + 4Q_{66}}{8} \\
U_2 &= \frac{Q_{11} - Q_{22}}{2} \\
U_3 &= \frac{Q_{11} + Q_{22} - 2Q_{12} - 4Q_{66}}{8} \\
U_4 &= \frac{Q_{11} + Q_{22} + 6Q_{12} - 4Q_{66}}{8} \\
U_5 &= \frac{Q_{11} + Q_{22} - 2Q_{12} + 4Q_{66}}{8}
\end{aligned} \tag{A.6}$$

Using the transformed stiffness matrix coefficient, the effective stiffness coefficient $\overline{b_{ij}}$ are calculated using the following equations.

$$b_{ij} = \frac{2}{h} \sum_{k=1}^{n/2} Q_{ijk} t_k \tag{A.7}$$

Where $n/2$ = Number of layers on either side of the mid plane of the symmetric

laminate

t_k = Thickness of individual layer

h = Total thickness of the laminate

The effective compliance coefficient are calculated as follows

$$\begin{aligned}
 \overline{a_{11}} &= \frac{\overline{b_{22}} \overline{b_{66}} - \overline{b_{26}^2}}{B} \\
 \overline{a_{12}} &= \frac{\overline{b_{16}} \overline{b_{26}} - \overline{b_{12}} \overline{b_{66}}}{B} \\
 \overline{a_{16}} &= \frac{\overline{b_{12}} \overline{b_{26}} - \overline{b_{16}} \overline{b_{22}}}{B} \\
 \overline{a_{22}} &= \frac{\overline{b_{11}} \overline{b_{66}} - \overline{b_{16}^2}}{B} \\
 \overline{a_{26}} &= \frac{\overline{b_{12}} \overline{b_{16}} - \overline{b_{11}} \overline{b_{26}}}{B} \\
 \overline{a_{66}} &= \frac{\overline{b_{11}} \overline{b_{22}} - \overline{b_{12}^2}}{B} \\
 B &= \overline{b_{11}} \overline{b_{22}} \overline{b_{66}} - \overline{b_{11}} \overline{b_{26}^2} + 2\overline{b_{12}} \overline{b_{26}} \overline{b_{16}} - \overline{b_{66}} \overline{b_{12}^2} - \overline{b_{22}} \overline{b_{16}^2}
 \end{aligned} \tag{A.8}$$

By introducing $\overline{a_{ij}}$ in the characteristics equation, the constant of anisotropy can be calculated for multilayered plates.

References

- [1] Jones Robert. *Mechanics of composite materials*. Taylor and Francis, Philadelphia, 1999.
- [2] Daniel Ori Ishai M.Isaac. *Engineering Mechanics of composite materials*.
- [3] Lekhnitskii S.G. *Anisotropic plates*. Gordon and Breach science publishers, New York, 1968.
- [4] Savin G.N. *Stress Concentration around Holes*. Pregamon Press, New York, 1961.
- [5] Muskhelishvili N.I. *Some Basic Problems of Mathematical Theory of Elasticity*. P.Noordhooft Ltd., The Netherlands, 1963.
- [6] Gao X.L. A general solution of an infinite elastic plate with an elliptic hole under biaxial loading. *International Journal of Pressure Vessels and Piping*, 67, pages 95–104, 1996.
- [7] Simha K.R.Y and Mohapatra S.S. Stress concentration around irregular holes using complex variable. *Sadhna (India)*, 23(4), pages 393–412, 1998.
- [8] Ukadgaonker V.G. and Awasare P.J. A novel method of stress analysis of an infinite plate with circular hole with uniform loading at infinity. *Indian Journal of Technology*, 31, pages 539–541, 1993.
- [9] Ukadgaonker V.G. and Awasare P.J. A novel method of stress analysis of an infinite plate with elliptical hole with uniform tensile stress. *Journal of the institution of Engineers (India), MC*, 73, pages 309–311, 1993.
- [10] Ukadgaonker V.G. and Rao D.K.N. A general solution for stresses around holes in symmetric laminates under in plane loading. *Journal of Composite Structures*, Vol.49, pages 339–354, 2000.
- [11] Ukadgaonker V.G. and Kakhandki Vyasraj. Stress analysis for an orthotropic plate with an irregular shaped hole for different in-plane loading conditions-part 1. *Journal of Composite Structures*, Vol.70, pages 255–274, 2005.

- [12] Sharma D.S. Stress analysis for an orthotropic plate with a circular hole subjected to in-plane loading. *Institute of Technology, Nirma University, Ahmedabad.*
- [13] Sharma D.S. Stress analysis of infinite orthotropic plate with an arbitrarily oriented crack subjected to inplane loading at infinity. *Institute of Technology, Nirma University, Ahmedabad.*
- [14] Sharma D.S. and Ukadgaonker V.G. Stress intensity factors for cracks emanating from a circular hole in laminated composite infinite plate under different loading conditions. *International Conference on Emerging Trends in Engineering and Technology.*
- [15] Ukadgaonker V.G. Interaction effect on stresses in plate with two unequal elliptical holes subjected to uniform tension at infinity. *Indian journal of Technology*, vol. 26, pages 549–559, 1988.
- [16] Ukadgaonker V.G. and Naik A.P. Interaction effect of two arbitrarily oriented cracks-part i. *International journal of fracture*, vol. 51, pages 219–230, 1991.
- [17] Ukadgaonker V.G. and Naik A.P. Effect of interaction of two arbitrarily oriented cracks-applications-part-ii. *International journal of fracture*, vol. 51, pages 285–304, 1991.
- [18] Cheong S.K. and Kwon O. N. Analysis of a crack approaching two circular holes in(0/90)s laminates. *Engg. fracture mechanics*, vol.-46, No.2, pages 235–244, 1993.
- [19] Lin J.K. and E.S.Ueng. Stresses in a laminated composite with two elliptical holes. *Composite Structure*, vol. 7, pages 1–20, 1987.
- [20] Sih G.C. and Liebowitz H. Mathematical theories of brittle fracture. *An advanced treatise*, vol. II, 1968.